

Supporting Information

Assessing the Metal-Metal Interactions in a Series of Heterobimetallic Nb/M Complexes (M = Fe, Co, Ni, Cu) and Their Effect on Multielectron Redox Properties

Brett A. Barden,[‡] Gursu Culcu,[†] Jeremy P. Krogman,[†] Mark W. Bezpalko,[†] Gregory P. Hatzis,[‡] Diane A. Dickie,[†] Bruce M. Foxman,[†] Christine M. Thomas^{*,†,‡}

[†] Department of Chemistry, Brandeis University, 415 South Street, Waltham, Massachusetts 02454, United States

[‡] Department of Chemistry and Biochemistry, The Ohio State University, 100 West 18th Avenue, Columbus, Ohio 43210, United States

Table of Contents

Figure S1	¹ H NMR spectrum of <i>i</i> PrN=Nb(μ -PPh ₂)(<i>i</i> PrNPPH ₂) ₂ Co-Br (3).	S4
Figure S2	¹ H NMR spectrum of Cl-Nb(<i>i</i> PrNPPH ₂) ₃ Ni-Cl (4).	S4
Figure S3	³¹ P{ ¹ H} NMR spectrum of Cl-Nb(<i>i</i> PrNPPH ₂) ₃ Ni-Cl (4).	S5
Figure S4	¹³ C{ ¹ H} NMR spectrum of Cl-Nb(<i>i</i> PrNPPH ₂) ₃ Ni-Cl (4).	S5
Figure S5	¹ H NMR spectrum of Cl-Nb(<i>i</i> PrNPPH ₂) ₃ Cu-Br (5).	S6
Figure S6	¹ H NMR spectrum of O≡Nb(<i>i</i> PrNPPH ₂) ₃ Fe-I (7).	S6
Figure S7	¹ H NMR spectrum of O≡Nb(<i>i</i> PrNPPH ₂) ₃ Co-I (8).	S7
Figure S8	¹ H NMR spectrum of O≡Nb(<i>i</i> PrNPPH ₂) ₃ Ni-Cl (9).	S7
Figure S9	¹ H NMR spectrum of O≡Nb(<i>i</i> PrNPPH ₂) ₃ Cu-I (10).	S8
Figure S10	³¹ P{ ¹ H} NMR spectrum of O≡Nb(<i>i</i> PrNPPH ₂) ₃ Cu-I (10).	S8
Figure S11	¹³ C{ ¹ H} NMR NMR spectrum of O≡Nb(<i>i</i> PrNPPH ₂) ₃ Cu-I (10).	S9
Figure S12	Cyclic voltammogram of Cl-Nb(<i>i</i> PrNPPH ₂) ₃ Fe-Br (2).	S9

Figure S13	Cyclic voltammogram of Cl-Nb(<i>i</i> PrNPPH ₂) ₃ Ni-Cl (4).	S10
Figure S14	Cyclic voltammogram of Cl-Nb(<i>i</i> PrNPPH ₂) ₃ Cu-Br (5).	S10
Figure S15	Cyclic voltammogram of O≡Nb(<i>i</i> PrNPPH ₂) ₃ (6).	S11
Figure S16	Cyclic voltammogram of O≡Nb(<i>i</i> PrNPPH ₂) ₃ Fe-I (7).	S11
Figure S17	Cyclic voltammogram of O≡Nb(<i>i</i> PrNPPH ₂) ₃ Co-I (8).	S12
Figure S18	Cyclic voltammogram of O≡Nb(<i>i</i> PrNPPH ₂) ₃ Ni-Cl (9).	S12
Figure S19	Cyclic voltammogram of O≡Nb(<i>i</i> PrNPPH ₂) ₃ Cu-I (10).	S13
Figure S20	EPR spectrum of O≡Nb(<i>i</i> PrNPPH ₂) ₃ Ni-Cl (9).	S13
Table S1	Crystallographic Data and Refinement Parameters for 3 , 4 , and 5 .	S14
Table S2	Crystallographic Data and Refinement Parameters for 7-10 .	S15
Figure S21	Fully labeled ellipsoid representation of 3 .	S16
	X-Ray data collection, solution, and refinement details for 3 .	S16-17
Figure S22	Fully labeled ellipsoid representation of 4 .	S18
	X-Ray data collection, solution, and refinement details for 4 .	S18-19
Figure S23	Fully labeled ellipsoid representation of 5 .	S20
	X-Ray data collection, solution, and refinement details for 5 .	S20-21
Figure S24	Fully labeled ellipsoid representation of 7 .	S22
	X-Ray data collection, solution, and refinement details for 7 .	S22-23
Figure S25	Fully labeled ellipsoid representation of 8 .	S24
	X-Ray data collection, solution, and refinement details for 8 .	S24-25
Figure S26	Fully labeled ellipsoid representation of 9 .	S26
	X-Ray data collection, solution, and refinement details for 9 .	S26-27
Figure S27	Fully labeled ellipsoid representation of 10 .	S28
	X-Ray data collection, solution, and refinement details for 10 .	S28
Table S3	Comparison of experimental and calculated bond metrics of 4 and 5 .	S29
Figure S28	Calculated frontier molecular orbital diagram of Cl-Nb(<i>i</i> PrNPPH ₂) ₃ Ni-Cl (4).	S29
Figure S29	Calculated frontier molecular orbital diagram of Cl-Nb(<i>i</i> PrNPPH ₂) ₃ Cu-Br (5).	S30
Table S4	Calculated XYZ coordinates for all atoms in 4 .	S31-33

Table S5	Calculated XYZ coordinates for all atoms in 5 .	S34-36
	References	S37

Figure S1. ^1H NMR (C_6D_6 , 400 MHz) spectrum of $^i\text{PrN}=\text{Nb}(\mu\text{-PPh}_2)(^i\text{PrNPPh}_2)_2\text{Co-Br}$ (**3**). Signals labeled as * correspond to residual solvent molecules, in this case THF, toluene, and Et_2O .

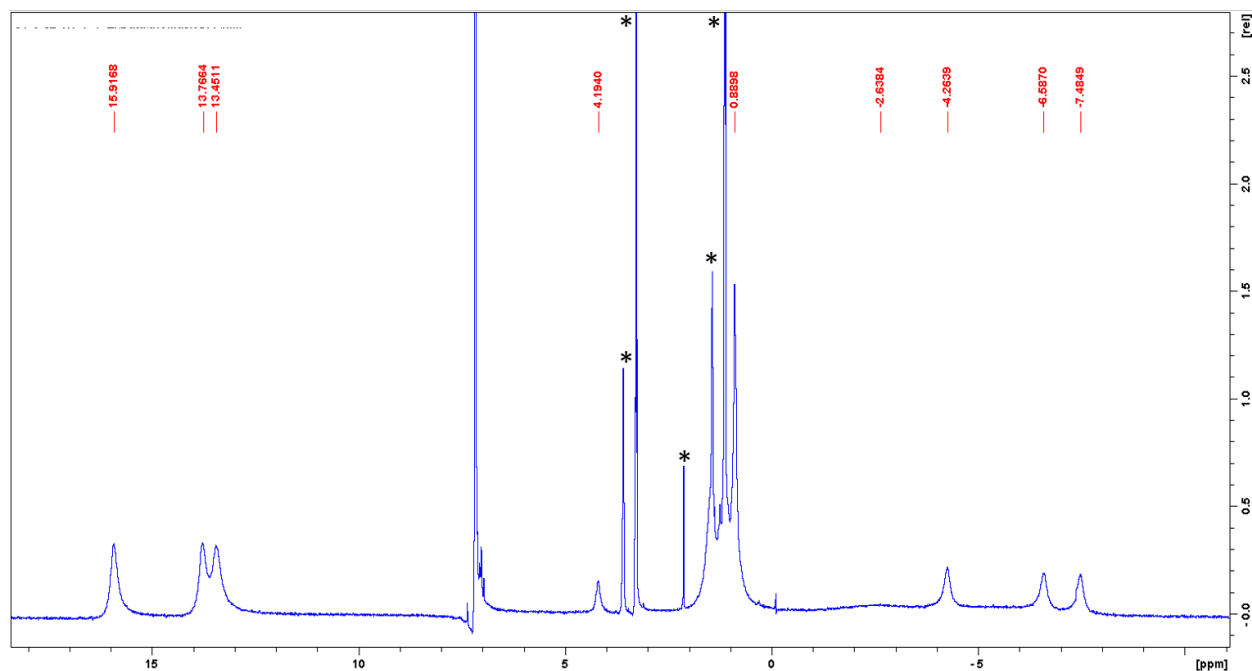


Figure S2. ^1H NMR (C_6D_6 , 400 MHz) spectrum of $\text{Cl-Nb}(^i\text{PrNPPh}_2)_3\text{Ni-Cl}$ (**4**). Signals labeled as * correspond to residual solvent molecules, in this case THF and pentane.

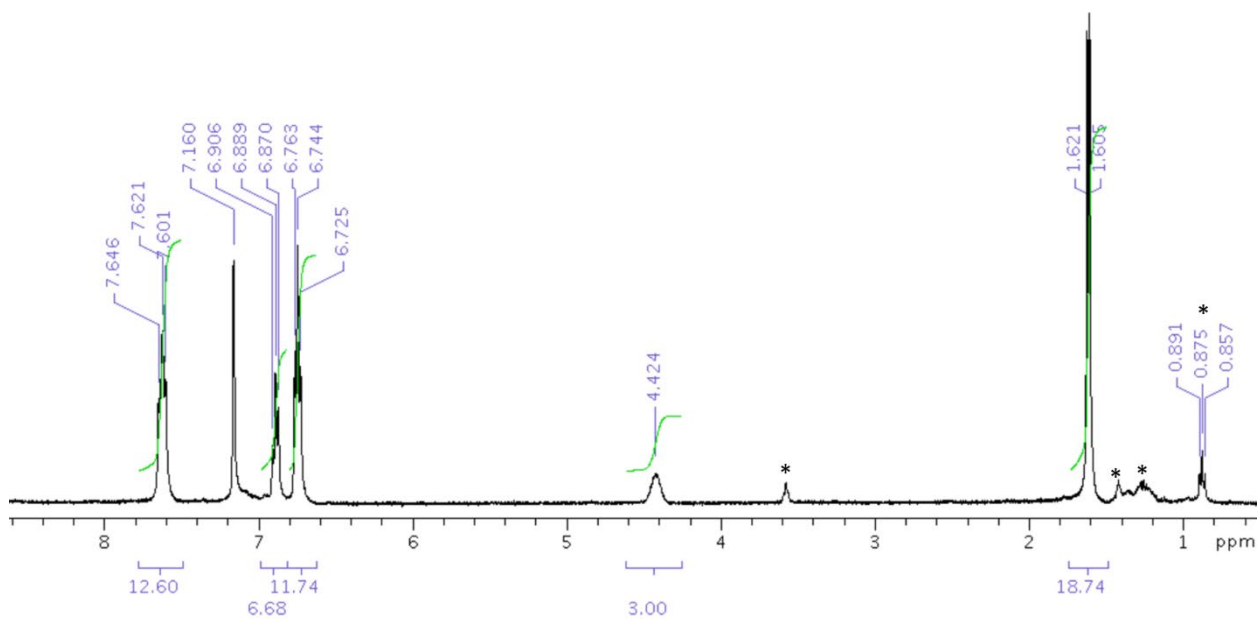


Figure S3. $^{31}\text{P}\{^1\text{H}\}$ NMR (C_6D_6 , 162 MHz) spectrum of $\text{Cl-Nb}(\text{}^i\text{PrNPh}_2)_3\text{Ni-Cl}$ (**4**).

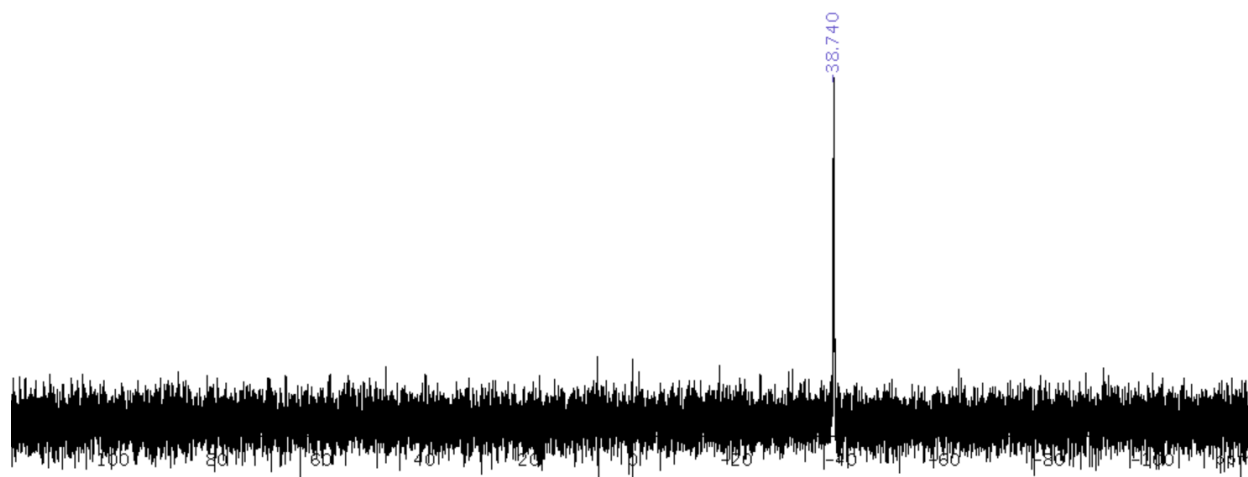


Figure S4. $^{13}\text{C}\{^1\text{H}\}$ NMR NMR (C_6D_6 , 100.6 MHz) spectrum of $\text{Cl-Nb}(\text{}^i\text{PrNPh}_2)_3\text{Ni-Cl}$ (**4**).

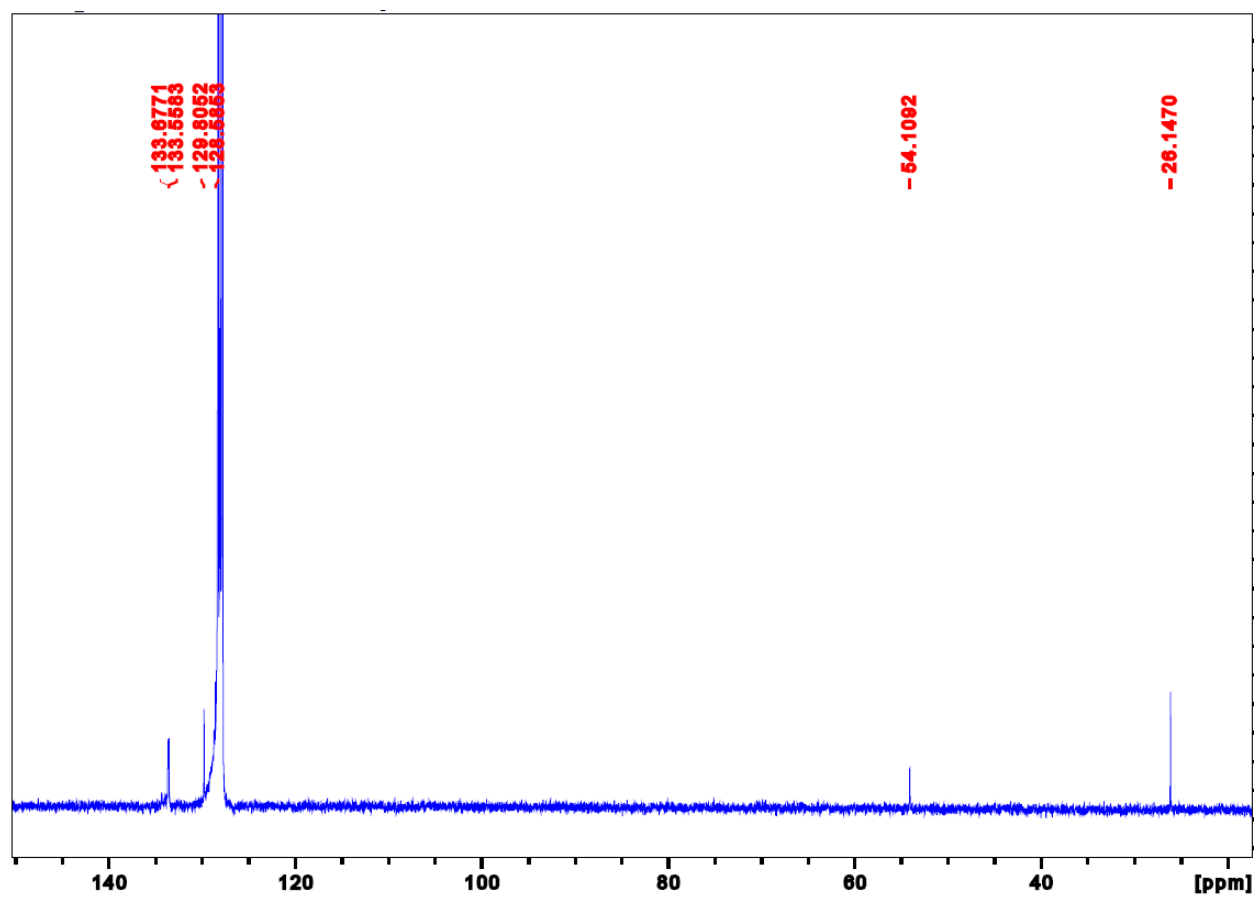


Figure S5. ^1H NMR (C_6D_6 , 400 MHz) spectrum of $\text{Cl-Nb}(\text{}^i\text{PrNPPH}_2)_3\text{Cu-Br}$ (**5**). Signals labeled as * correspond to residual solvent molecules, in this case pentane, THF and $\text{C}_6\text{D}_5\text{H}$.

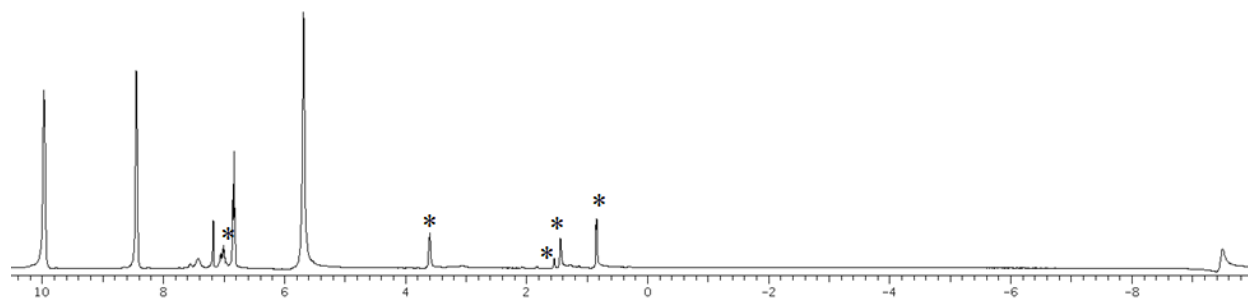


Figure S6. ^1H NMR (C_6D_6 , 400 MHz) spectrum of $\text{O}\equiv\text{Nb}(\text{}^i\text{PrNPPH}_2)_3\text{Fe-I}$ (**7**). Signals labeled as * correspond to residual solvent molecules, in this case Et_2O , hexanes, and $\text{C}_6\text{D}_5\text{H}$.

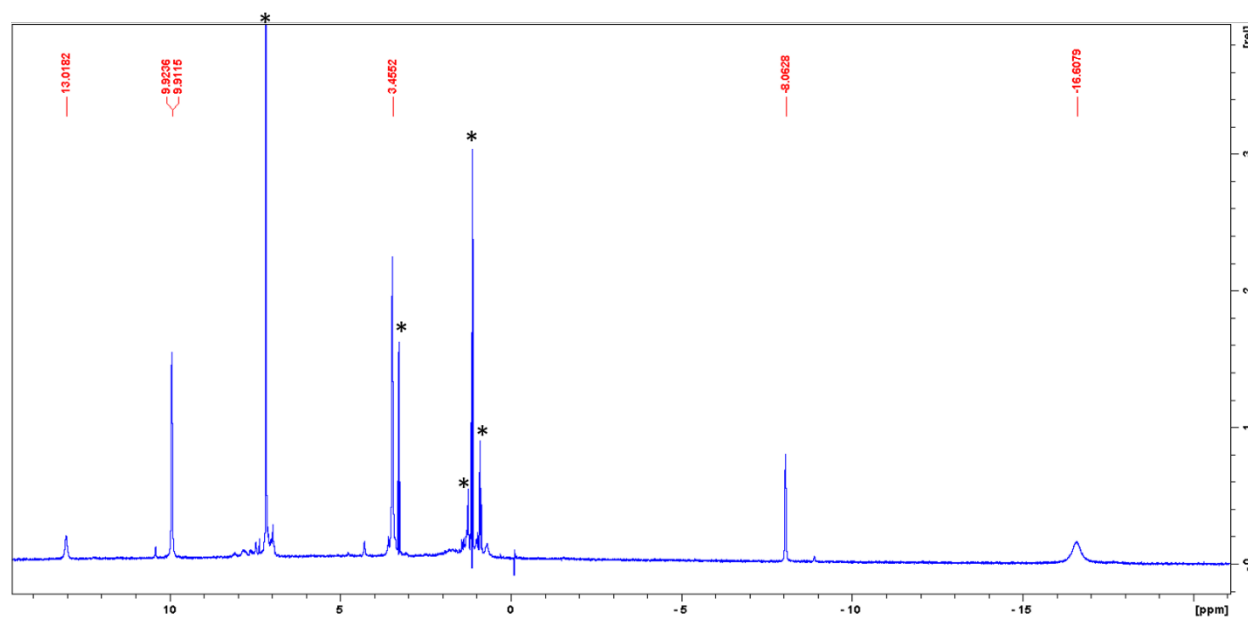


Figure S7. ^1H NMR (C_6D_6 , 400 MHz) spectrum of $\text{O}\equiv\text{Nb}(\text{}^i\text{PrNPPH}_2)_3\text{Co-I}$ (**8**). Signals labeled as * correspond to residual solvent molecules, in this case THF and $\text{C}_6\text{D}_5\text{H}$.

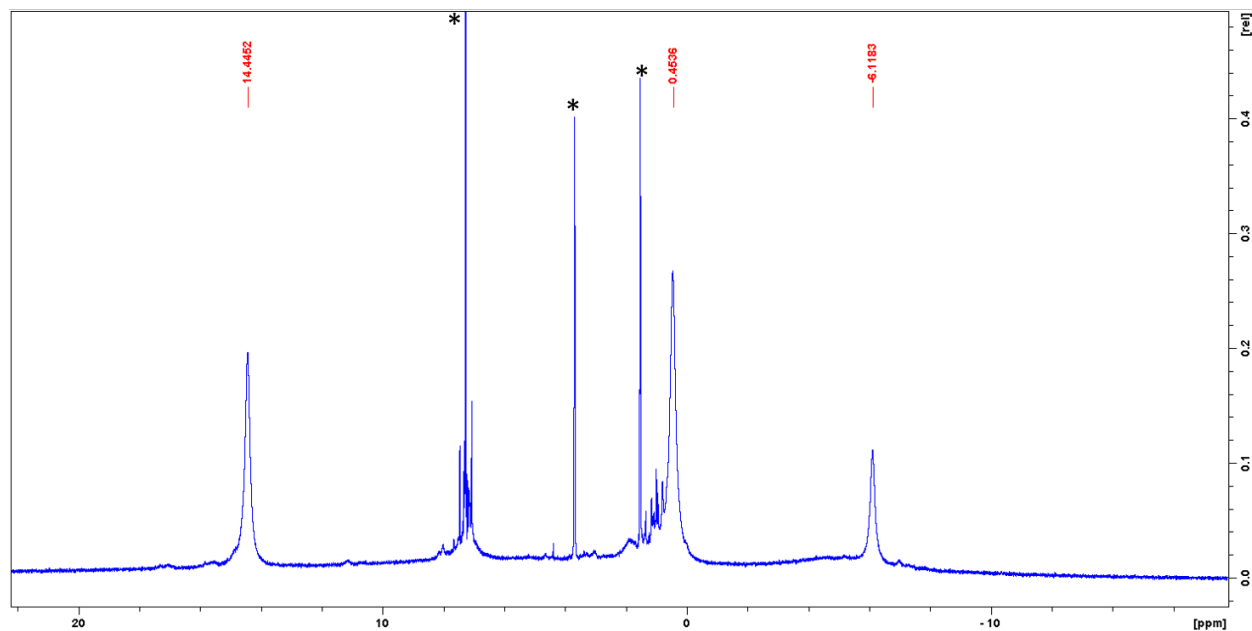


Figure S8. ^1H NMR (C_6D_6 , 400 MHz) spectrum of $\text{O}\equiv\text{Nb}(\text{}^i\text{PrNPPH}_2)_3\text{Ni-Cl}$ (**9**). Signals labeled as * correspond to residual solvent molecules, in this case $\text{C}_6\text{D}_5\text{H}$.

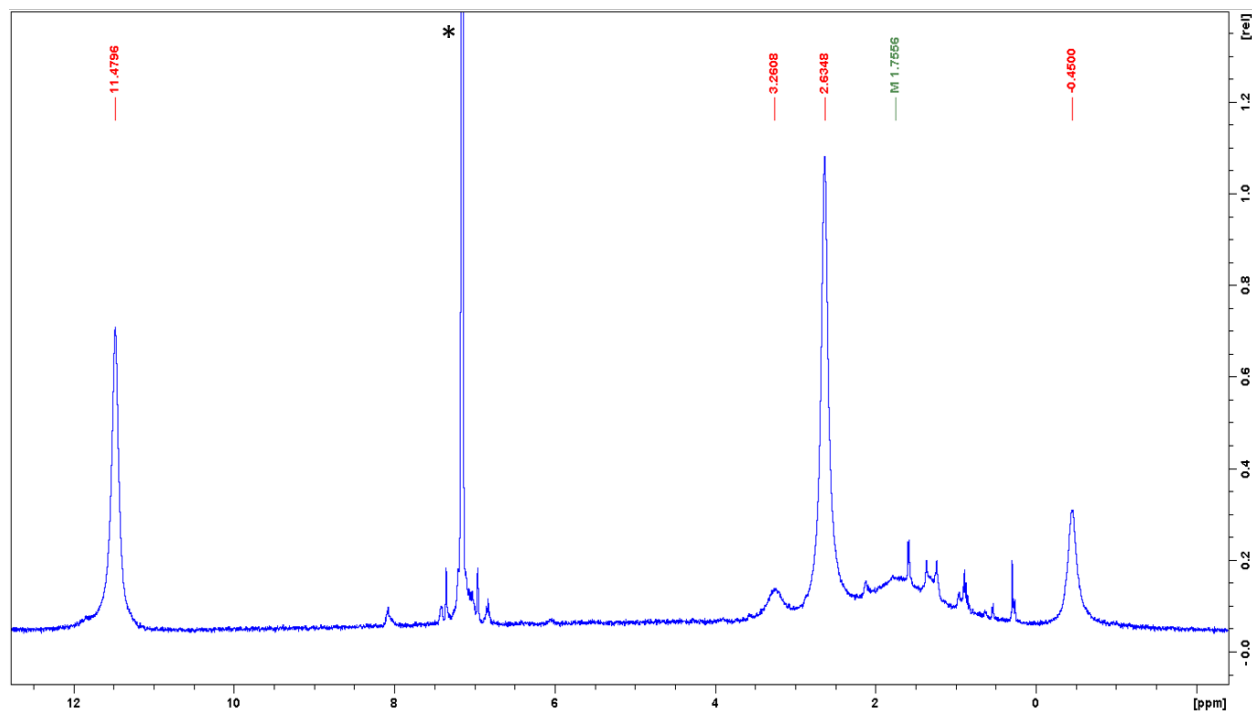


Figure S9. ^1H NMR (CD_2Cl_2 , 400 MHz) spectrum of $\text{O}\equiv\text{Nb}(\text{}^i\text{PrNPPh}_2)_3\text{Cu-I}$ (**10**).

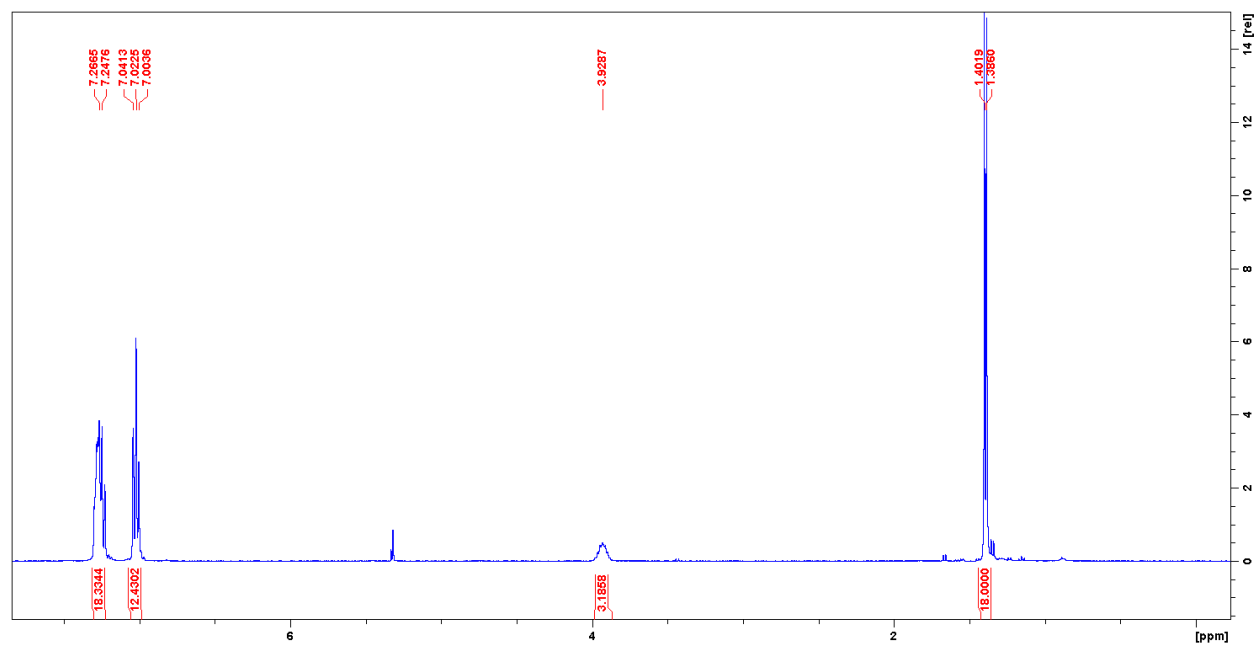


Figure S10. $^{31}\text{P}\{^1\text{H}\}$ NMR (CD_2Cl_2 , 162 MHz) spectrum of $\text{O}\equiv\text{Nb}(\text{}^i\text{PrNPPh}_2)_3\text{Cu-I}$ (**10**).

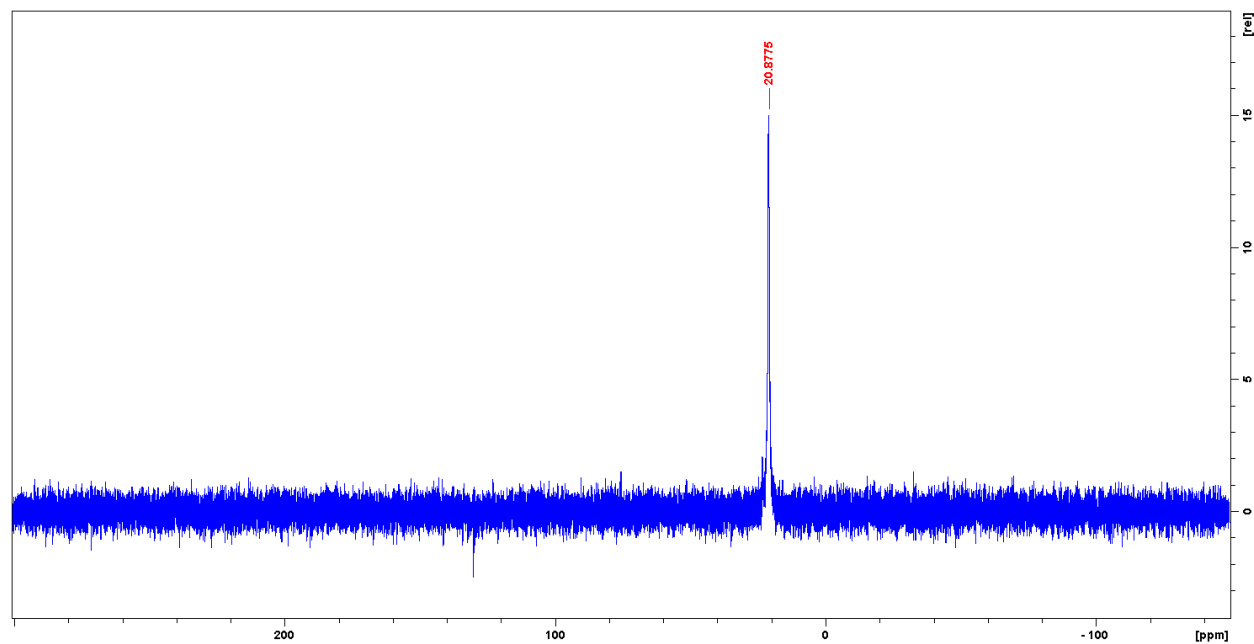


Figure S11. $^{13}\text{C}\{^1\text{H}\}$ NMR NMR (CD_2Cl_2 , 100.6 MHz) spectrum of $\text{O}\equiv\text{Nb}(\text{}^i\text{PrNPPH}_2)_3\text{Cu-I}$ (**10**).

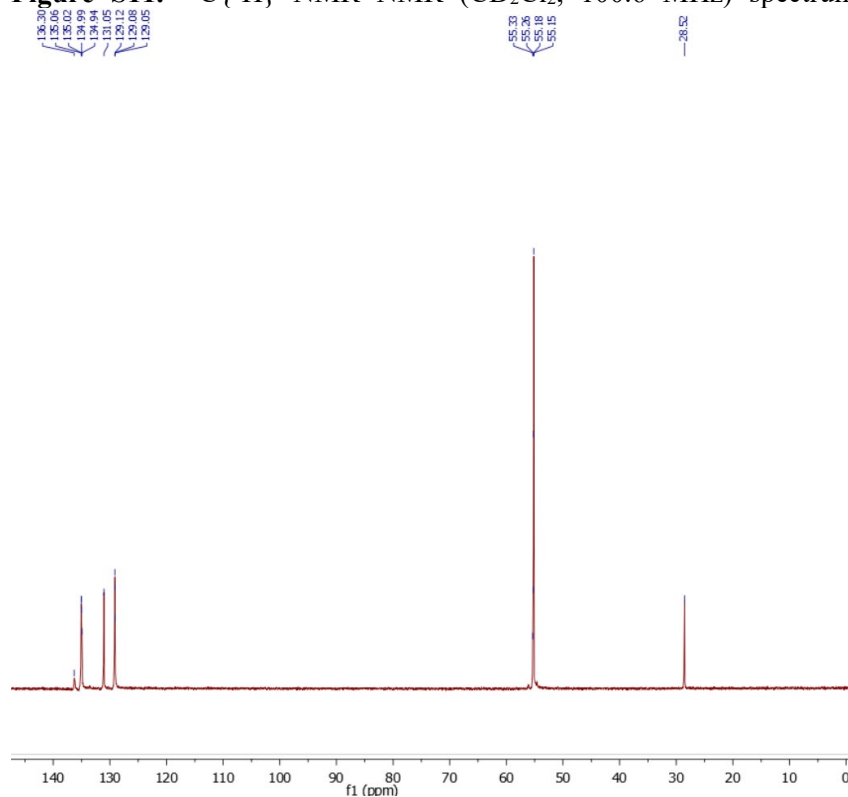


Figure S12. Cyclic voltammogram of $\text{Cl-Nb}(\text{}^i\text{PrNPPH}_2)_3\text{Fe-Br}$ (**2**) in 0.3 M $[\text{}^n\text{Bu}_4\text{N}][\text{PF}_6]$ in THF (scan rate = 100 mV/s) at different potential ranges. Inset : Scan rate dependence of the one-electron reduction process, revealing quasi-reversible behavior.

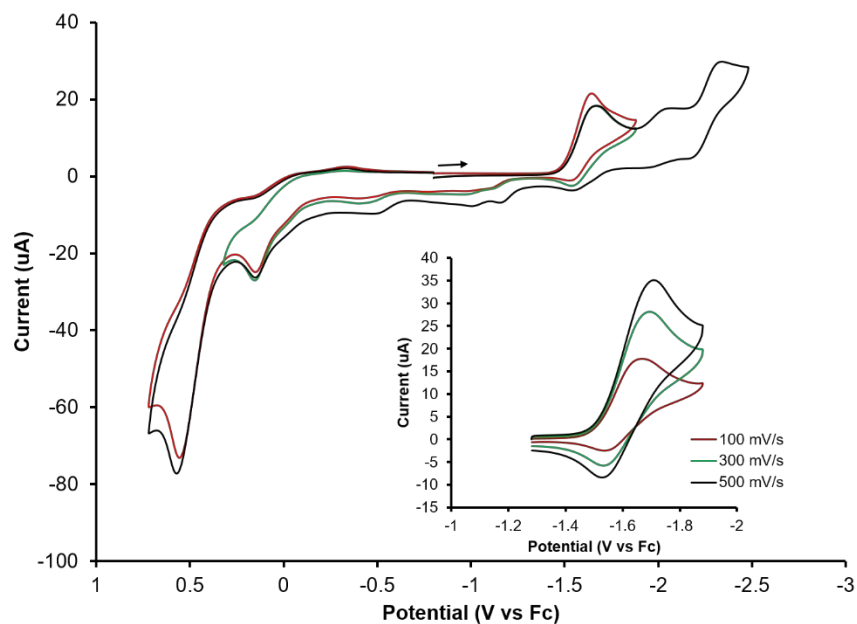


Figure S13. Cyclic voltammogram of Cl-Nb(*i*PrNPh₂)₃Ni-Cl (**4**) in 0.3 M [ⁿBu₄N][PF₆] in THF (scan rate = 100 mV/s) at different potential ranges and scan directions. Inset : Scan rate dependence of the one-electron reduction process, revealing quasi-reversible behavior.

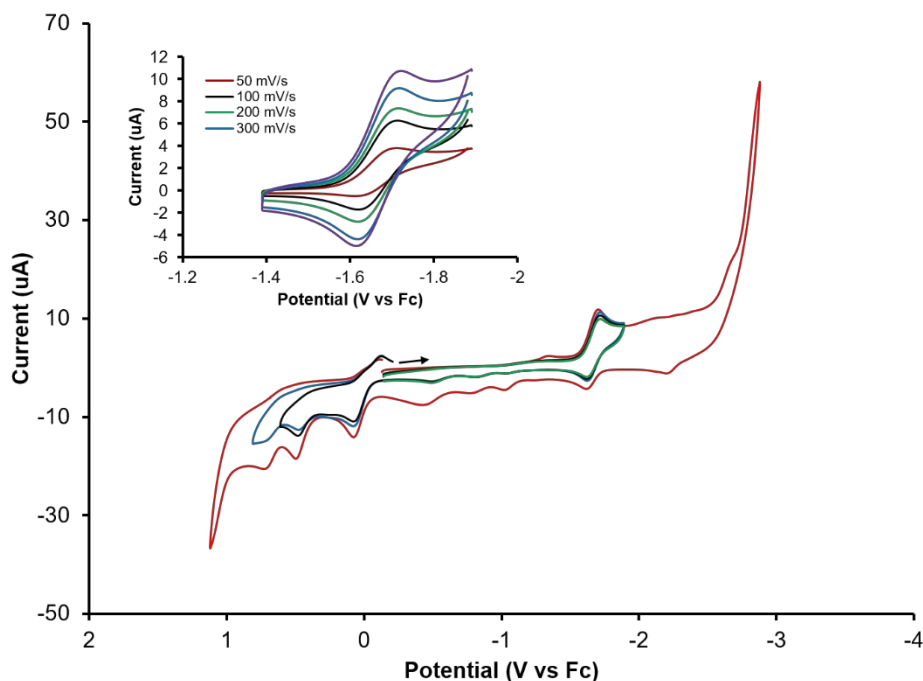


Figure S14. Cyclic voltammogram of Cl-Nb(*i*PrNPh₂)₃Cu-Br (**5**) in 0.3 M [ⁿBu₄N][PF₆] in THF (scan rate = 100 mV/s) at different potential ranges and scan directions.

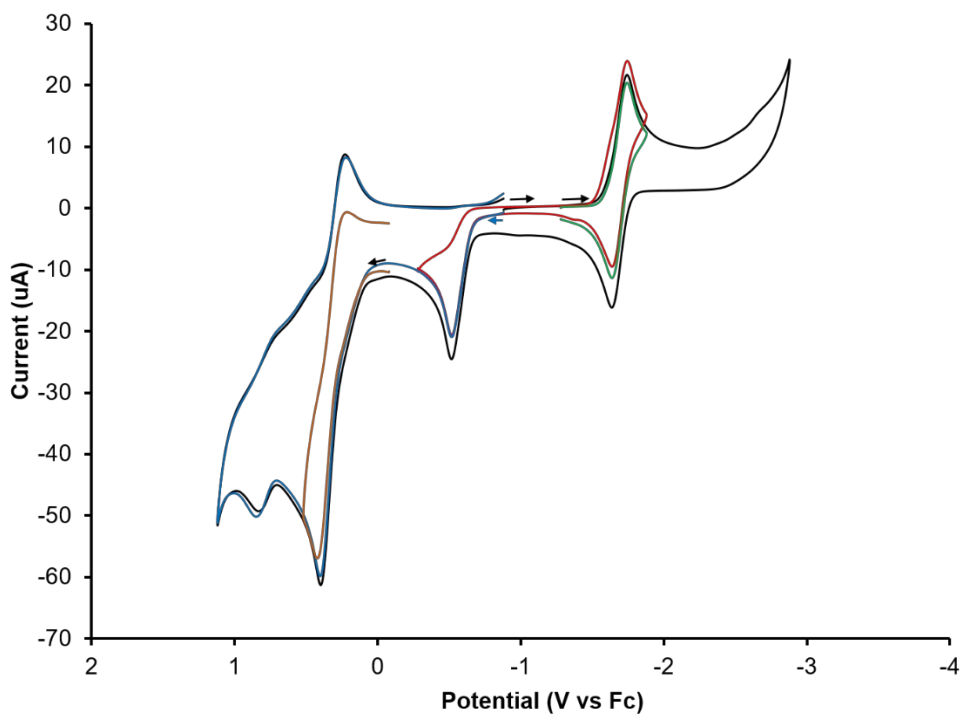


Figure S15. Cyclic voltammogram of $\text{O}\equiv\text{Nb}(\text{}^i\text{PrNPPH}_2)_3$ (**6**) in 0.3 M $[\text{}^n\text{Bu}_4\text{N}][\text{PF}_6]$ in THF (scan rate = 100 mV/s).

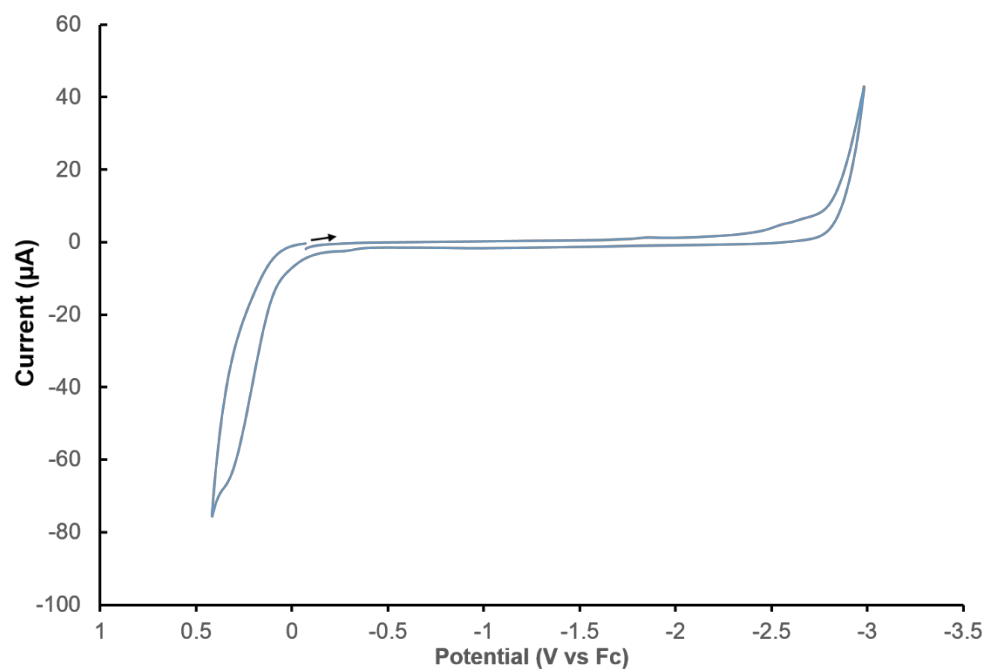


Figure S16. Cyclic voltammogram of $\text{O}\equiv\text{Nb}(\text{}^i\text{PrNPPH}_2)_3\text{Fe-I}$ (**7**) in 0.3 M $[\text{}^n\text{Bu}_4\text{N}][\text{PF}_6]$ in THF (scan rate = 100 mV/s) at different potential ranges.

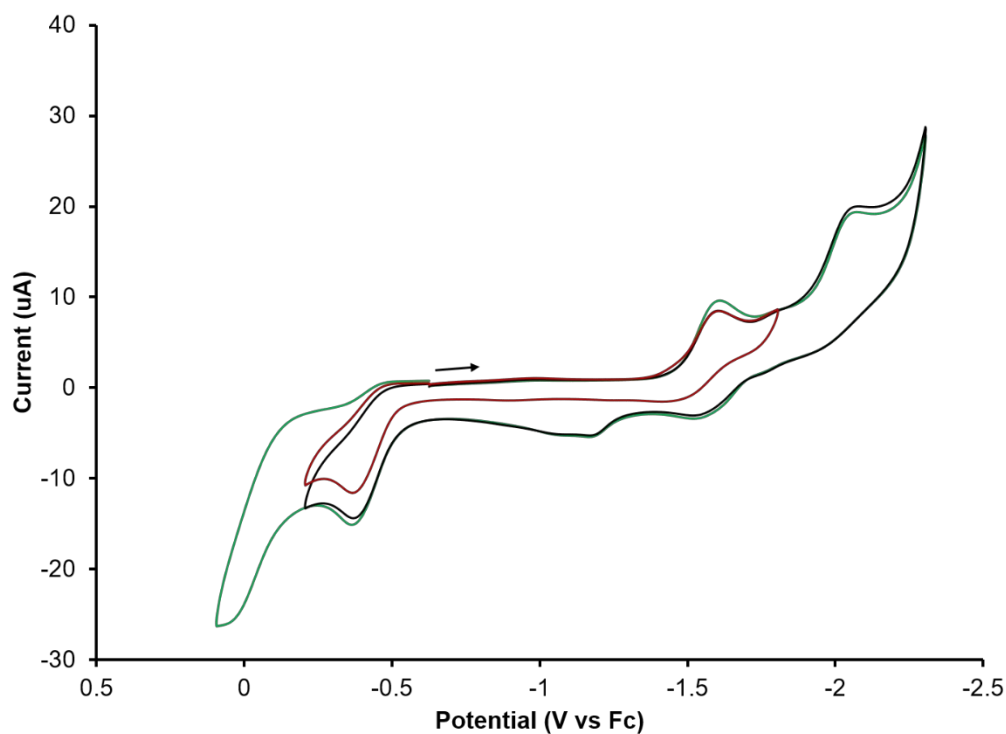


Figure S17. Cyclic voltammogram of $\text{O}\equiv\text{Nb}(\text{}^i\text{PrNPPH}_2)_3\text{Co-I}$ (**8**) in 0.3 M $[\text{}^n\text{Bu}_4\text{N}][\text{PF}_6]$ in THF (scan rate = 100 mV/s) at different potential ranges and scan directions. Insets : Scan rate dependence of the one-electron reduction and oxidation process, revealing quasi-reversible behavior.

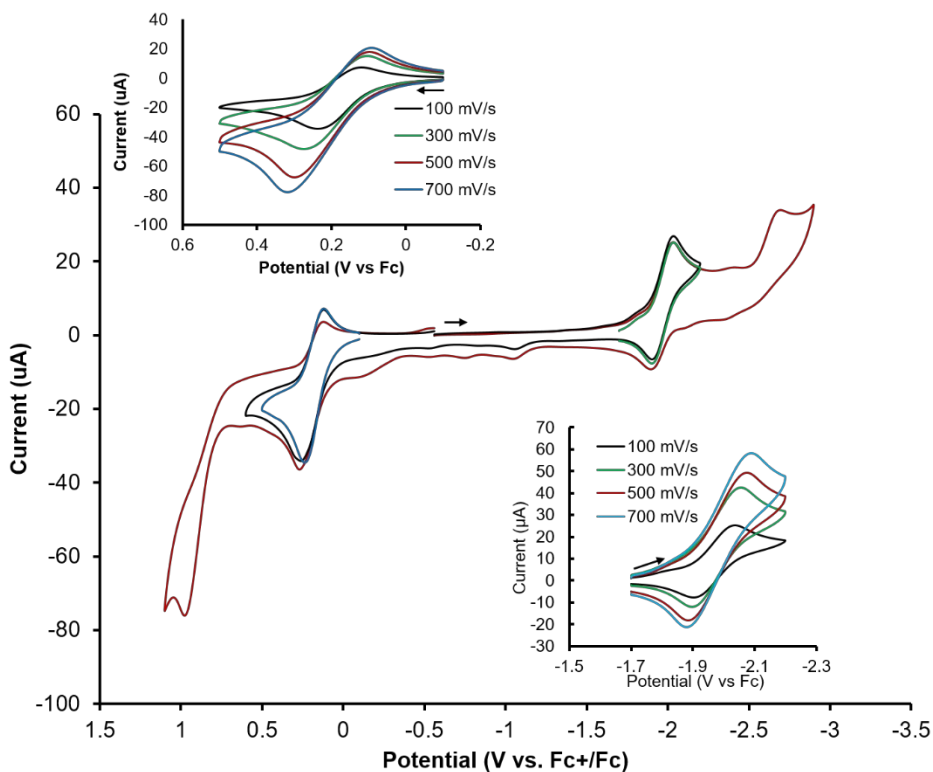


Figure S18. Cyclic voltammogram of $\text{O}\equiv\text{Nb}(\text{}^i\text{PrNPPH}_2)_3\text{Ni-Cl}$ (**9**) in 0.3 M $[\text{}^n\text{Bu}_4\text{N}][\text{PF}_6]$ in THF (scan rate = 100 mV/s) at different potential ranges.

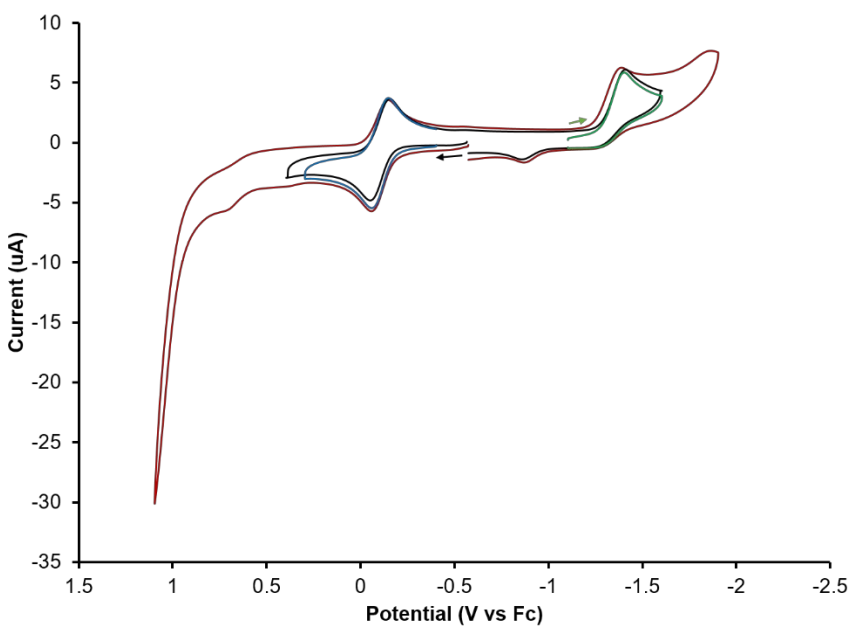


Figure S19. Cyclic voltammogram of $\text{O}\equiv\text{Nb}(\text{}^i\text{PrNPPH}_2)_3\text{Cu-I}$ (**10**) in 0.3 M $[\text{}^n\text{Bu}_4\text{N}][\text{PF}_6]$ in THF (scan rate = 100 mV/s) at different potential ranges.

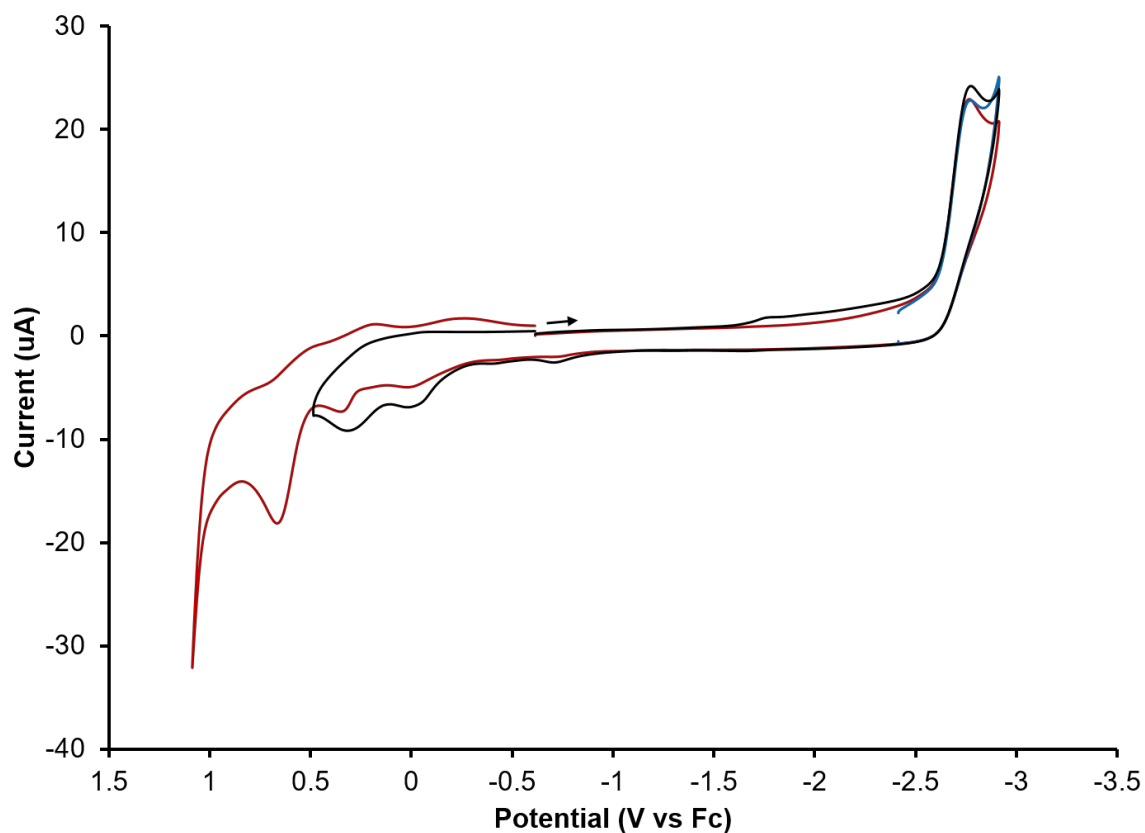


Figure S20. X-band EPR spectrum of $\text{O}\equiv\text{Nb}(\text{}^i\text{PrNPPH}_2)_3\text{Ni-Cl}$ (**9**) in frozen toluene (30 K, 9.38 GHz, 5 G modulation amplitude, 30 dB).

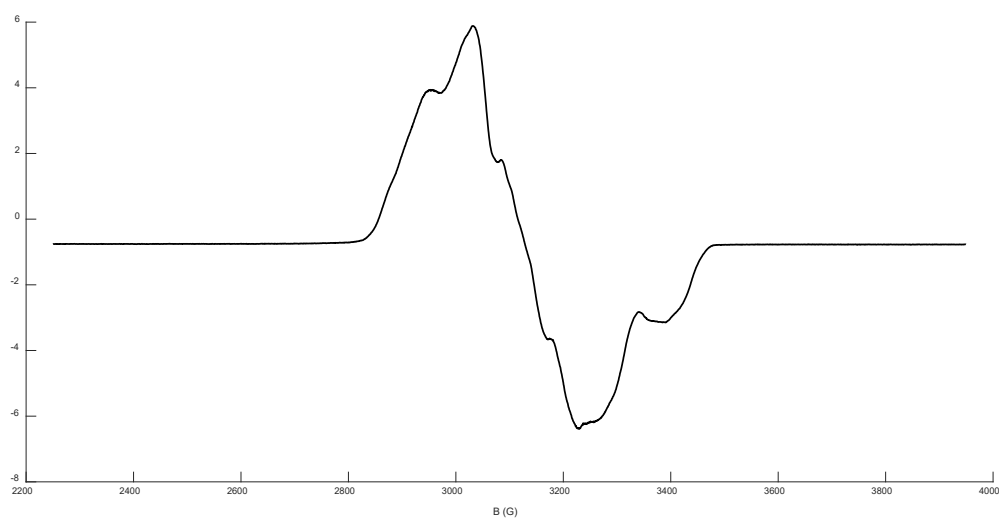


Table S1. Crystallographic Data and Refinement Parameters for **3**, **4**, and **5**.

	3 •toluene	4	5 •2THF
chemical formula	C ₅₂ H ₅₉ BrCoN ₃ NbP ₃	C ₄₅ H ₅₁ Cl ₂ N ₃ NbNiP	C ₅₃ H ₆₇ BrClCuN ₃ NbO ₂ P ₃
fw	1050.68	949.32	1142.86
<i>T</i> (K)	150	120	120
λ (Å)	0.71073	0.71073	0.71073
<i>a</i> (Å)	10.6062(8)	13.6692(3)	21.9645(8)
<i>b</i> (Å)	16.8558(12)	21.8518(6)	18.7834(7)
<i>c</i> (Å)	31.1162(18)	18.0145(5)	25.3941(11)
α (deg)	90	90	90
β (deg)	93.773(2)	108.1730(10)	90
γ (deg)	90	90	90
<i>V</i> (Å ³)	5550.8(7)	5112.4(2)	10476.8(7)
space group	<i>P</i> 2 ₁ / <i>c</i>	<i>P</i> 2 ₁ / <i>n</i>	<i>Pbca</i>
<i>Z</i> , <i>Z'</i>	4, 1	4, 1	8, 1
<i>D</i> _{calc} (g/cm ³)	1.257	1.233	1.449
μ (cm ⁻¹)	13.45	8.21	15.72
<i>R</i> ₁ (<i>I</i> > 2 σ (<i>I</i>)), w <i>R</i> ₂ ^a (all)	0.0506, 0.1280	0.0361, 0.0887	0.0447, 0.1033

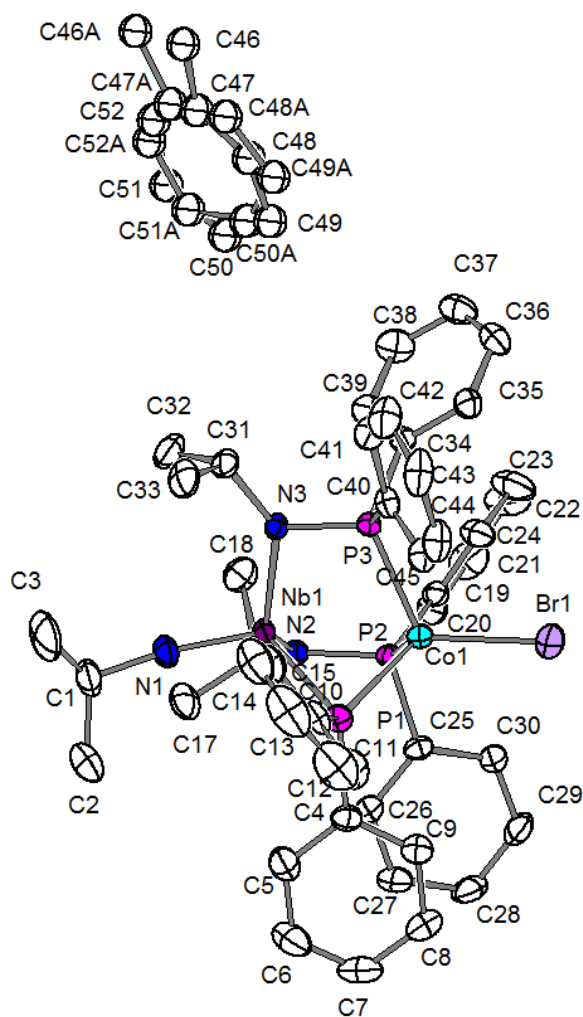
$$^a R_1 = \sum ||F_o| - |F_c|| / \sum |F_o|; wR_2 = \{ \sum [w(F_o^2 - F_c^2)_2] / \sum [w(F_o^2)^2] \}^{1/2}.$$

Table S2. Crystallographic Data and Refinement Parameters for **7-10**.

	7 •3CH ₂ Cl ₂	8	9	10
chemical formula	C ₄₈ H ₅₇ Cl ₆ FeIN ₃ NbOP ₃	C ₄₅ H ₅₁ CoIN ₃ NbOP ₃	C ₄₅ H ₅₁ N ₃ OP ₃ ClNiNb	C ₄₅ H ₅₁ CuIN ₃ NbOP ₃
fw	1273.23	1021.58	929.86	1026.20
<i>T</i> (K)	120	120	150	120
λ (Å)	0.71073	0.71073	0.71073	0.71073
<i>a</i> (Å)	23.3909(6)	20.6864(9)	20.6284(6)	20.7296(8)
<i>b</i> (Å)	18.4415(5)	20.6864(9)	20.6284(6)	20.7296(8)
<i>c</i> (Å)	25.3602(6)	20.6864(9)	20.6284(6)	20.7296(8)
α (deg)	90	90	90	90
β (deg)	90	90	90	90
γ (deg)	90	90	90	90
<i>V</i> (Å ³)	10939.5(5)	8852.3(7)	8778.0(8)	8907.8(10)
space group	<i>Pbca</i>	<i>Pa</i> $\bar{3}$	<i>Pa</i> $\bar{3}$	<i>Pa</i> $\bar{3}$
<i>Z</i> , <i>Z'</i>	8,1	8, 1/3	8, 1/3	8, 1/3
<i>D</i> _{calc} (g/cm ³)	1.546	1.533	1.407	1.530
μ (cm ⁻¹)	14.57	14.77	8.98	15.73
R ₁ (<i>I</i> > 2 σ (<i>I</i>)), wR ₂ ^a (all)	0.0365, 0.0785	0.0251, 0.0583	0.0243, 0.0638	0.0304, 0.0739

$$^a R_1 = \sum ||F_o| - |F_c|| / \sum |F_o|; wR_2 = \{ \sum [w(F_o^2 - F_c^2)_2] / \sum [w(F_o^2)^2] \}^{1/2}.$$

Figure S21. Fully labeled ellipsoid representation of **3**.



X-Ray data collection, solution, and refinement details for **3.**

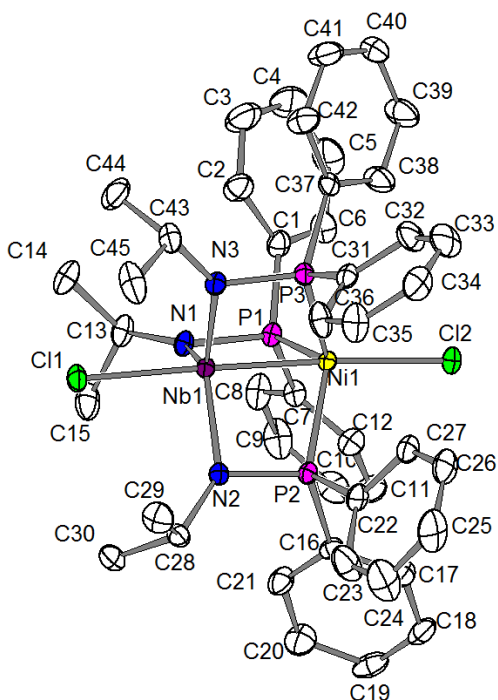
A red plate-like sample of $C_{45}H_{51}N_3P_3CoBrNb$ of approximate dimensions 0.24 x 0.12 x 0.08 mm was coated with Paratone oil and mounted on a MiTeGen MicroLoop that was previously attached to a metallic pin mechanically. The X-ray intensity data were measured on a Bruker D8 Venture PHOTON II CPAD system equipped with a graphite monochromator and a Mo $K\alpha$ fine-focus tube ($\lambda = 0.71073 \text{ \AA}$).

A total of 1910 frames were collected. The frames were integrated with the Bruker SAINT software package¹ using a narrow-frame algorithm. Using a monoclinic unit cell, the integration yielded 109801 reflections to a maximum θ angle of 27.536° (0.77 \AA resolution), of which 12719 were independent (redundancy = 10.10, completeness = 99.46%, $R_{\text{int}} = 6.03\%$, $R_{\text{sigma}} = 3.53\%$) and 10330 (81.21%) were greater than $2\sigma(F^2)$. The unit cell constants of $a = 10.6062(8)$, $b = 16.8558(12)$, $c = 31.1162(18)$, $\beta = 93.773(2)^\circ$ and $V = 5550.8(7) \text{ \AA}^3$ are based upon the refinement of the XYZ-centroids of 9712 reflections above $20 \sigma(I)$ with $6.176^\circ \leq 2\theta \leq 55.012^\circ$. Data were corrected for absorption effects with the Multi-Scan method (SADABS).¹ The ratio of minimum to maximum apparent transmission was 0.883, and the calculated minimum and maximum transmission coefficients (based on crystal size) are 0.738 and 0.900.

The structure was solved and refined with the Bruker SHELXTL Software Package² within APEX3¹ and Olex2³ using the space group $P2_1/c$, $Z=4$ and the formula $C_{45}H_{51}N_3P_3CoBrNb$. Ordered Non-hydrogen atoms were refined anisotropically. One toluene solvent was found to be fully disordered and was

refined isotropically. This was modeled with two-component disorder, where the sum of the major and minor components was constrained to be one. EADP constraints were used on the thermal displacement parameters of the disordered atoms and DFIX, DANG, and SADI restraints were used on the bonds of the toluene. Hydrogen atoms were placed in geometrically calculated positions with $U_{iso} = 1.2U_{equiv}$ of the parent atom ($U_{iso} = 1.5U_{equiv}$ for methyl). The final anisotropic full-matrix least-squares refinement converged at $R_1 = 5.06\%$ for the observed data and $wR_2 = 12.80\%$ for all the data. The goodness of fit is 1.025. The largest peak in the final electron density synthesis is $2.51 \text{ e } \text{\AA}^{-3}$ and the largest hole is $-1.67 \text{ e } \text{\AA}^{-3}$ with an average deviation of $0.101 \text{ e } \text{\AA}^{-3}$. Based on the final model, the calculated density is 1.257 g cm^{-3} and $F(000)$ is 2160 e^- . During the refinement, it became clear that the reflections corresponding to the Miller indices (0,1,4) were affected by the shadow of the beamstop (error = 21.11). There is one B-level alert in the Checkcif that corresponds to the beamstop location, and the long c-axis of the unit cell. This was confirmed by independently viewing the frames that the reflection appeared in, so these reflections have been omitted from the solution and refinement. Electron density difference maps revealed that there was disordered solvent that could not be successfully modeled, so the structure factors were modified using the PLATON SQUEEZE⁴ technique. PLATON reported a total electron density of 180 e^- and total solvent accessible volume of 972 \AA^3 , likely representing 8 toluene molecules per unit cell.

Figure S22. Fully labeled ellipsoid representation of **4**.



X-Ray data collection, solution, and refinement details for **4.**

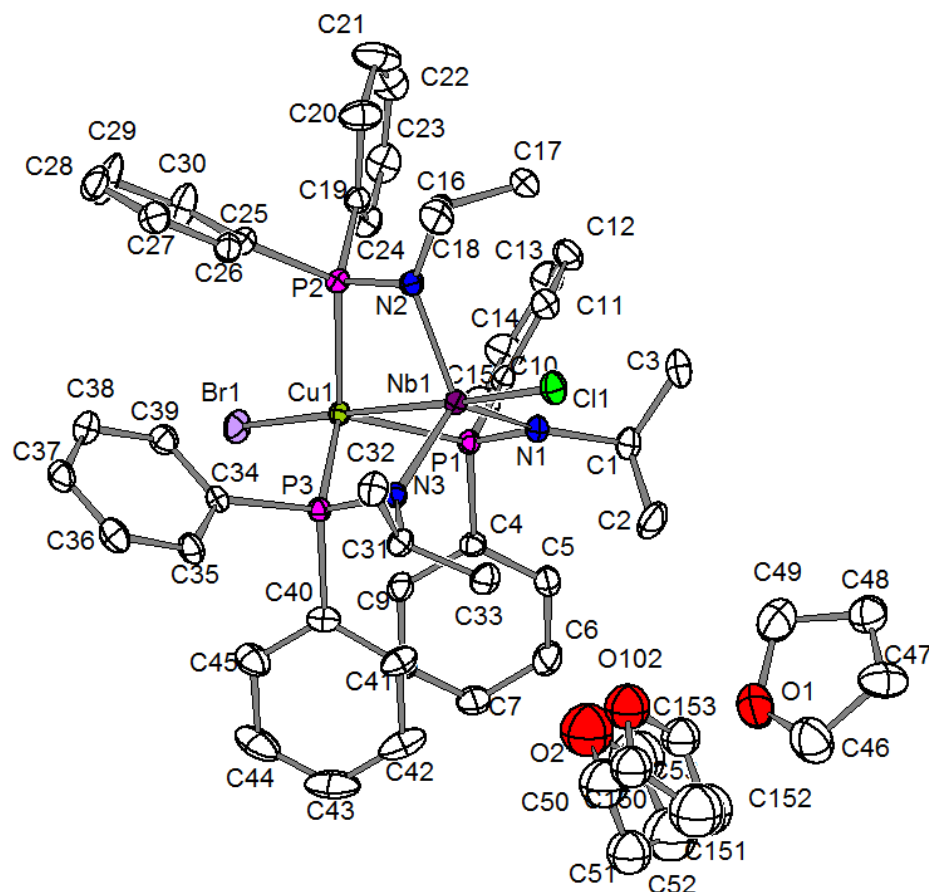
A red block-like specimen of $C_{45}H_{51}Cl_2N_3NbNiP_3$, approximate dimensions 0.190 mm x 0.233 mm x 0.294 mm, was coated with Paratone oil and mounted on a MiTeGen MicroLoop that had been previously attached to a metallic pin using epoxy for the X-ray crystallographic analysis. The X-ray intensity data were measured on a Bruker Kappa APEX II CCD system equipped with a graphite monochromator and a Mo $K\alpha$ fine-focus tube ($\lambda = 0.71073 \text{ \AA}$).

The total exposure time was 4.04 hours. A total of 1455 frames were collected. The frames were integrated with the Bruker SAINT software package¹ using a narrow-frame algorithm. The integration of the data using a monoclinic unit cell yielded a total of 54160 reflections to a maximum θ angle of 28.34° (0.75 \AA resolution), of which 12701 were independent (average redundancy 4.264, completeness = 99.6%, $R_{\text{int}} = 4.61\%$, $R_{\text{sig}} = 4.74\%$) and 9516 (74.92%) were greater than $2\sigma(F^2)$. The final cell constants of $a = 13.6692(3) \text{ \AA}$, $b = 21.8518(6) \text{ \AA}$, $c = 18.0145(5) \text{ \AA}$, $\beta = 108.1730(10)^\circ$, volume = $5112.5(2) \text{ \AA}^3$, are based upon the refinement of the XYZ-centroids of 9960 reflections above $20 \sigma(I)$ with $4.422^\circ < 2\theta < 56.46^\circ$. Data were corrected for absorption effects using the Multi-Scan method (SADABS).¹ The ratio of minimum to maximum apparent transmission was 0.810. The calculated minimum and maximum transmission coefficients (based on crystal size) are 0.7940 and 0.8600.

The structure was solved and refined using the Bruker SHELXTL Software Package² within APEX3¹ and OLEX2,³ using the space group $P 2_1/n$, with $Z = 4$ for the formula unit, $C_{45}H_{51}Cl_2N_3NbNiP_3$. Non-hydrogen atoms were refined anisotropically. Hydrogen atoms were placed in geometrically calculated positions with $U_{\text{iso}} = 1.2U_{\text{equiv}}$ of the parent atom ($U_{\text{iso}} = 1.5U_{\text{equiv}}$ for methyl). During the structure solution, electron density difference maps revealed that there was disordered solvent that could not be successfully modeled. Thus, the structure factors were modified using the PLATON SQUEEZE⁴ technique, in order to produce a “solvate-free” structure factor set. PLATON reported a total electron density of $235 e^-$ and total solvent accessible volume of 1088 \AA^3 , likely representing 6-8 diethyl ether molecules per unit cell. The final anisotropic full-matrix least-squares refinement on F^2 with 502 variables converged at $R1 = 3.61\%$,

for the observed data and $wR2 = 8.87\%$ for all data. The goodness-of-fit was 1.032. The largest peak in the final difference electron density synthesis was $0.902 \text{ e}/\text{\AA}^3$ and the largest hole was $-0.727 \text{ e}/\text{\AA}^3$ with an RMS deviation of $0.076 \text{ e}/\text{\AA}^3$. On the basis of the final model, the calculated density was $1.233 \text{ g}/\text{cm}^3$ and $F(000)$, 1960 e^- .

Figure S23. Fully labeled ellipsoid representation of **5**.



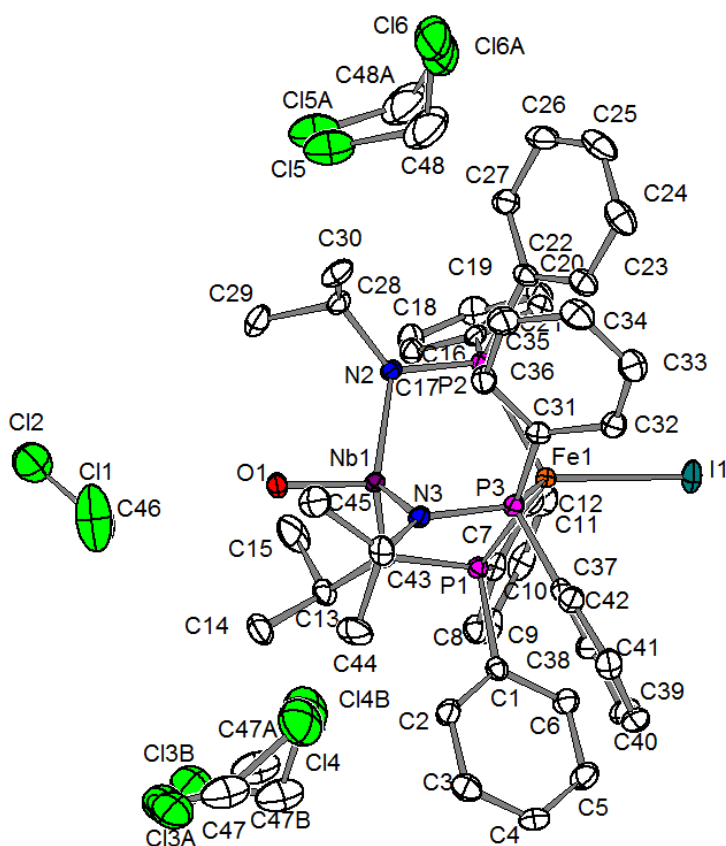
X-Ray data collection, solution, and refinement details for **5.**

All operations were performed on a Bruker-Nonius Kappa Apex2 diffractometer, using graphite-monochromated MoK α radiation. All diffractometer manipulations, including data collection, integration, scaling, and absorption corrections were carried out using the Bruker Apex2 software.⁵ Preliminary cell constants were obtained from three sets of 12 frames. Data collection was carried out at 120 K, using a frame time of 10 sec and a detector distance of 60 mm. The optimized strategy used for data collection consisted of three phi and three omega scan sets, with 0.5° steps in phi or omega; completeness was 99.9 %. A total of 1137 frames were collected. Final cell constants were obtained from the xyz centroids of 8554 reflections after integration.

From the systematic absences, the observed metric constants and intensity statistics, space group *Pbca* was chosen initially; subsequent solution and refinement confirmed the correctness of this choice. The structure was solved using *SIR-92*,⁶ and refined (full-matrix-least squares) using the Oxford University *Crystals for Windows* program.⁷⁻⁸ The asymmetric unit contains one molecule of the complex and two tetrahydrofuran solvates (for the complex, *Z* = 8; *Z'* = 1). All ordered non-hydrogen atoms were refined using anisotropic displacement parameters. After location of H atoms on electron-density difference maps, the H atoms were initially refined with soft restraints on the bond lengths and angles to regularize their geometry (C---H in the range 0.93--0.98 Å and *U*_{iso} (H) in the range 1.2-1.5 times *U*_{eq} of the parent atom), after which the positions were refined with riding constraints.⁹ One of the THF solvates were found to be fully disordered; the disorder was modeled as a two-component disorder. Occupancies of major/minor component atoms were constrained to sum to 1.0. The components and their occupancies are: [O(2),C(50,51,52,53)/ O(102),C(150,151,152,153); 0.454/0.546(6)]. All the modeled disordered

components were refined using isotropic displacement parameters. Distance and angle restraints were applied to the disordered atoms. The final least-squares refinement converged to $R_1 = 0.0447$ ($I > 2\sigma(I)$, 10007 data) and $wR_2 = 0.1033$ (F^2 , 15266 data, 582 parameters). The final CIF is available as supporting material.

Figure S24. Fully labeled ellipsoid representation of 7.



X-Ray data collection, solution, and refinement details for 7.

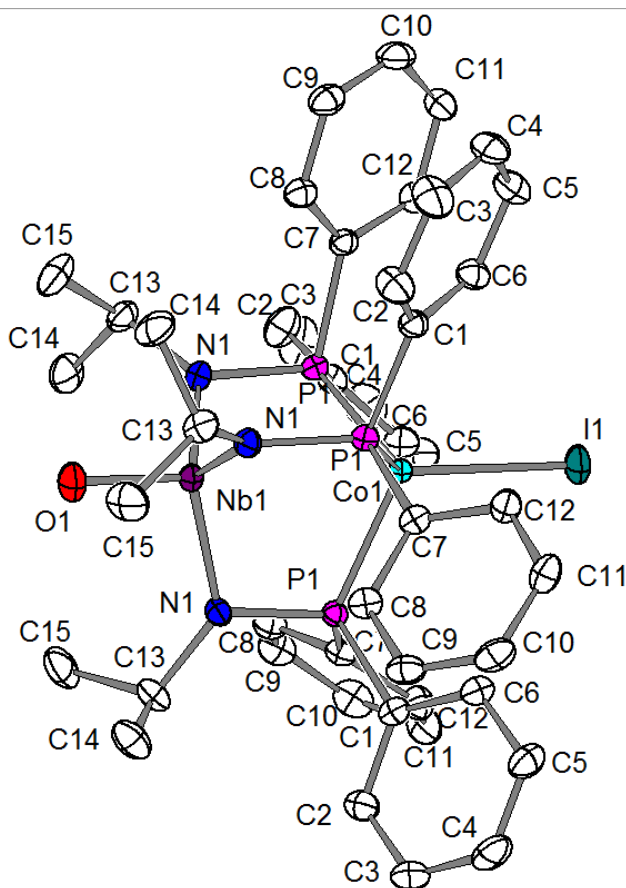
A red plate-like specimen of $C_{48}H_{57}Cl_6FeIN_3NbOP_3$, approximate dimensions 0.072 mm x 0.326 mm x 0.382 mm, was coated with Paratone oil and mounted on a MiTeGen MicroLoop that had been previously attached to a metallic pin using epoxy for the X-ray crystallographic analysis. The X-ray intensity data were measured on a Bruker Kappa APEX II CCD system equipped with a graphite monochromator and a Mo $K\alpha$ fine-focus tube ($\lambda = 0.71073 \text{ \AA}$).

The total exposure time was 5.30 hours. A total of 1271 frames were collected. The frames were integrated with the Bruker SAINT software package¹ using a narrow-frame algorithm. The integration of the data using an orthorhombic unit cell yielded a total of 93255 reflections to a maximum θ angle of 27.50° (0.77 \AA resolution), of which 12550 were independent (average redundancy 7.431, completeness = 99.9%, $R_{\text{int}} = 6.54\%$, $R_{\text{sig}} = 5.07\%$) and 9034 (71.98%) were greater than $2\sigma(F^2)$. The final cell constants of $a = 23.3909(6) \text{ \AA}$, $b = 18.4415(5) \text{ \AA}$, $c = 25.3602(6) \text{ \AA}$, volume = $10939.5(5) \text{ \AA}^3$, are based upon the refinement of the XYZ-centroids of 9881 reflections above $20 \sigma(I)$ with $4.425^\circ < 2\theta < 53.39^\circ$. Data were corrected for absorption effects using the Multi-Scan method (SADABS).¹ The ratio of minimum to maximum apparent transmission was 0.751. The calculated minimum and maximum transmission coefficients (based on crystal size) are 0.6060 and 0.9020.

The structure was solved and refined using the Bruker SHELXTL Software Package² within APEX3¹ and OLEX2,³ using the space group Pbc_a , with $Z = 8$ for the formula unit, $C_{48}H_{57}Cl_6FeIN_3NbOP_3$. Non-hydrogen atoms were refined anisotropically. Hydrogen atoms, were placed in geometrically calculated positions with $U_{\text{iso}} = 1.2U_{\text{equiv}}$ of the parent atom ($U_{\text{iso}} = 1.5 U_{\text{equiv}}$ for methyl).

One CH₂Cl₂ solvent was found to be disordered over two positions, while another was disordered over three positions. The relative occupancies of the disordered positions were freely refined, with a SUMP instruction on the three-component disorder to assure the fragments summed to one. EADP constraints were used on the thermal displacement parameters of the disordered atoms, with DFIX restraints on the C47-Cl4 and C47B-Cl4B distances. The final anisotropic full-matrix least-squares refinement on F² with 614 variables converged at R1 = 3.65%, for the observed data and wR2 = 7.85% for all data. The goodness-of-fit was 1.013. The largest peak in the final difference electron density synthesis was 0.989 e⁻/Å³ and the largest hole was -0.965 e⁻/Å³ with an RMS deviation of 0.105 e⁻/Å³. On the basis of the final model, the calculated density was 1.546 g/cm³ and F(000), 5128 e⁻.

Figure S25. Fully labeled ellipsoid representation of **8**.



X-Ray data collection, solution, and refinement details for **8.**

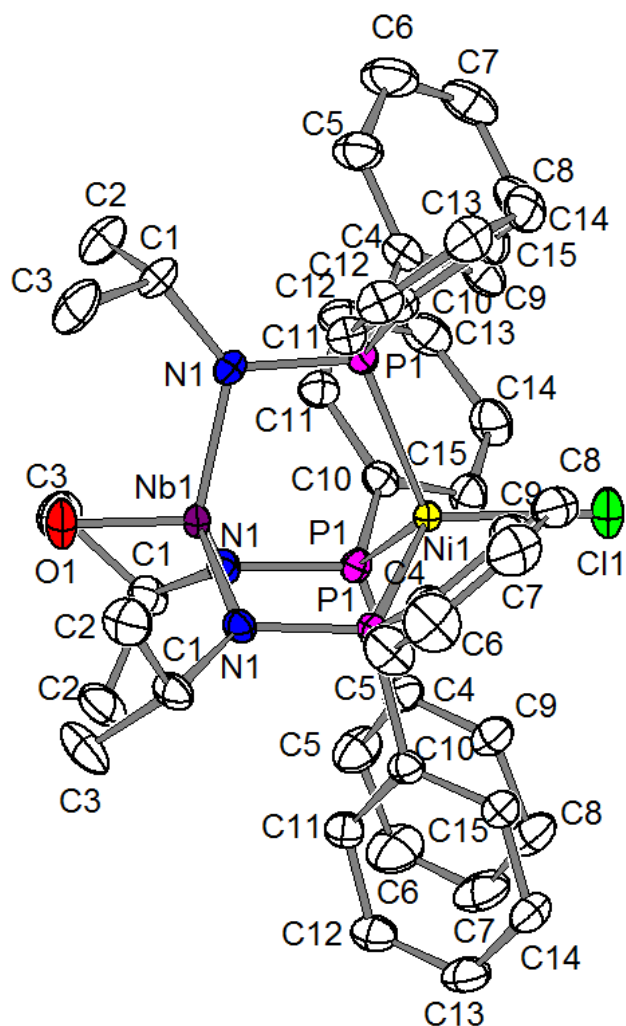
All operations were performed on a Bruker-Nonius Kappa Apex2 diffractometer, using graphite-monochromated MoK α radiation. All diffractometer manipulations, including data collection, integration, scaling, and absorption corrections were carried out using the Bruker Apex2 software.⁵ Preliminary cell constants were obtained from three sets of 12 frames. Data collection was carried out at 120 K, using a frame time of 20 sec and a detector distance of 60 mm. The optimized strategy used for data collection consisted of one phi and three omega scan sets, with 0.5° steps in phi or omega; completeness was 99.9%. A total of 604 frames were collected. Final cell constants were obtained from the xyz centroids of 8765 reflections after integration.

From the systematic absences, the observed metric constants and intensity statistics, space group

$Pa\bar{3}$ was chosen initially; subsequent solution and refinement confirmed the correctness of this choice. The structure was solved using the coordinates of the isomorphous Hf analogue, ClHf(ⁱPrNPPPh₂)₃CoI,¹⁰ and simply changing the identity of the Hf atom to Nb and Cl atom to O. The structure was solved using *SuperFlip*,¹¹ and refined (full-matrix-least squares) using the Oxford University *Crystals for Windows* program.⁷⁻⁸ All non-hydrogen atoms were refined using anisotropic displacement parameters. After location of H atoms on electron-density difference maps, the H atoms were initially refined with soft restraints on the bond lengths and angles to regularize their geometry (C---H in the range 0.93--0.98 Å and U_{iso} (H) in the range 1.2-1.5 times U_{eq} of the parent atom), after which the positions were refined with riding constraints.⁹ The final least-squares refinement converged to $R_1 = 0.0251$ ($I > 2\sigma(I)$, 3526 data) and $wR_2 = 0.0583$ (F^2 , 4312 data, 166 parameters). The final CIF is available as supporting material; CheckCIF reported one Alert B error, related to differences in the evaluation software's calculation of s.u.'s in the

absence of variance/covariance information. Accordingly, the CIF contains a validation reply form item which addresses this issue.

Figure S26. Fully labeled ellipsoid representation of **9**.



X-Ray data collection, solution, and refinement details for **9.**

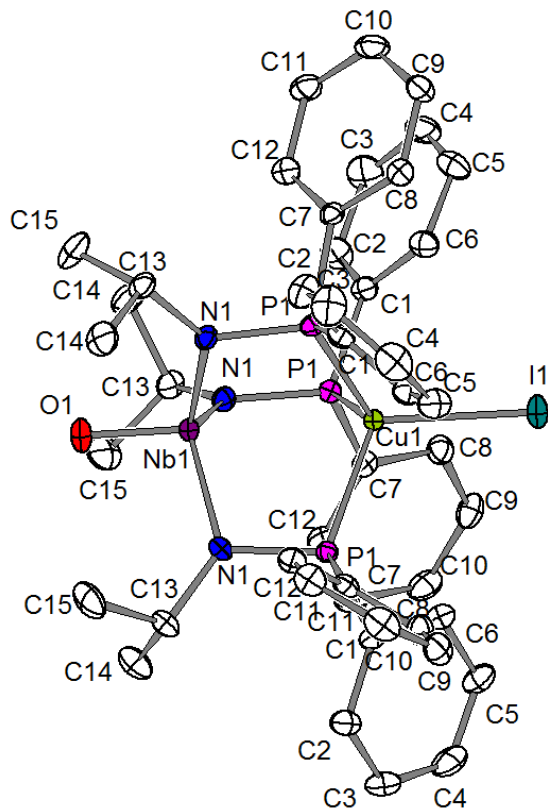
A yellow plate-like sample of $C_{45}H_{51}N_3OP_3ClNiNb$ of approximate dimensions 0.538 x 0.288 x 0.26 mm was coated with Paratone oil and mounted on a MiTeGen MicroLoop that was previously attached to a metallic pin mechanically. The X-ray intensity data were measured on a Bruker D8 Venture PHOTON II CPAD system equipped with a graphite monochromator and a Mo $K\alpha$ fine-focus tube ($\lambda = 0.71073 \text{ \AA}$).

A total of 900 frames were collected. The frames were integrated with the Bruker SAINT software package¹ using a narrow-frame algorithm. Using a cubic unit cell, the integration yielded 113006 reflections to a maximum θ angle of 30.5° (0.70 \AA resolution), of which 4471 were independent (redundancy = 40.83, completeness = 99.85%, $R_{\text{int}} = 2.74\%$, $R_{\text{sigma}} = 0.85\%$) and 4103 (91.77%) were greater than $2\sigma(F^2)$. The unit cell constants of $a = 20.6284(6)$, $V = 8778.0(8) \text{ \AA}^3$ are based upon the refinement of the XYZ-centroids of 9654 reflections above $20 \sigma(I)$ with $5.586^\circ \leq 2\theta \leq 61^\circ$. Data were corrected for absorption effects with the Multi-Scan method (SADABS).¹ The ratio of minimum to maximum apparent transmission was 0.844, and the calculated minimum and maximum transmission coefficients (based on crystal size) are 0.7410 and 0.7920.

The structure was solved and refined with the Bruker SHELXTL Software Package² within APEX3¹ and Olex2³ using the space group Pa-3, $Z=8$ and the formula $C_{45}H_{51}N_3OP_3ClNiNb$. Non-hydrogen atoms were refined anisotropically. Hydrogen atoms were placed in geometrically calculated positions with

$U_{iso} = 1.2U_{equiv}$ of the parent atom ($U_{iso} = 1.5U_{equiv}$ for methyl). The final anisotropic full-matrix least-squares refinement converged at $R1 = 2.43\%$ for the observed data and $wR2 = 6.38\%$ for all the data. The goodness of fit is 1.074. The largest peak in the final electron density synthesis is $0.68 \text{ e } \text{\AA}^{-3}$ and the largest hole is $-0.52 \text{ e } \text{\AA}^{-3}$ with an average deviation of $0.053 \text{ e } \text{\AA}^{-3}$. Based on the final model, the calculated density is 1.407 g cm^{-3} and $F(000)$ is 3848 e⁻. During the refinement, it became clear that the reflections corresponding to the Miller indices (1,2,2) were affected by the shadow of the beamstop (error = 12.86). This was confirmed by independently viewing the frames that the reflection appeared in, so these reflections have been omitted from the solution and refinement.

Figure S27. Fully labeled ellipsoid representation of **10**.



X-Ray data collection, solution, and refinement details for 10.

All operations were performed on a Bruker-Nonius Kappa Apex2 diffractometer, using graphite-monochromated MoK α radiation. All diffractometer manipulations, including data collection, integration, scaling, and absorption corrections were carried out using the Bruker Apex2 software.⁵ Preliminary cell constants were obtained from three sets of 12 frames. Data collection was carried out at 120K, using a frame time of 10 sec and a detector distance of 60 mm. The optimized strategy used for data collection consisted of one phi and two omega scan sets, with 0.5° steps in phi or omega; completeness was 100 %. A total of 392 frames were collected. Final cell constants were obtained from the xyz centroids of 8803 reflections after integration.

From the systematic absences, the observed metric constants and intensity statistics, space group $Pa\bar{3}$ was chosen initially; subsequent solution and refinement confirmed the correctness of this choice. The structure was solved using *SuperFlip*,¹¹ and refined (full-matrix-least squares) using the Oxford University *Crystals for Windows* program.⁷⁻⁸ The asymmetric unit contains a third molecule of the complex ($Z = 8$; $Z' = 1/3$). All non-hydrogen atoms were refined using anisotropic displacement parameters. After location of H atoms on electron-density difference maps, the H atoms were initially refined with soft restraints on the bond lengths and angles to regularize their geometry (C---H in the range 0.93--0.98 Å and U_{iso} (H) in the range 1.2-1.5 times U_{eq} of the parent atom), after which the positions were refined with riding constraints.⁹ The final least-squares refinement converged to $R_1 = 0.0304$ ($I > 2\sigma(I)$, 3588 data) and $wR_2 = 0.0739$ (F^2 , 4354 data, 166 parameters). The final CIF is available as supporting material.

Table S3. Comparison of experimental (X-Ray) and calculated (DFT, Gaussian)¹² bond metrics of **4** and **5**. Experimental and calculated bond lengths are in Ångstroms (Å).

	4		5	
	Exp.	Calc.	Exp.	Calc.
Nb-M	2.2990(3)	2.37	2.6572(4)	2.76
Nb-N (avg.)	2.03(2)	2.07	2.04(2)	2.07
M-P (avg.)	2.23(6)	2.26	2.31(8)	2.35

Figure S28. Calculated frontier molecular orbital diagram of Cl-Nb(ⁱPrNPh₂)₃Ni-Cl (**4**).

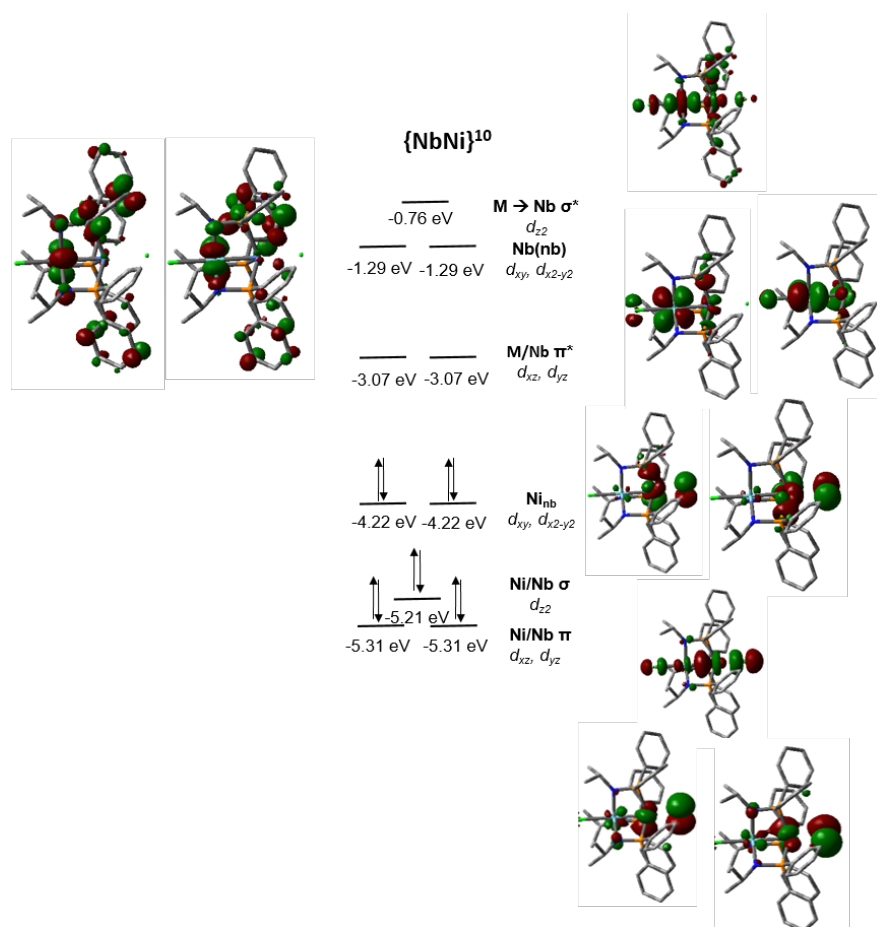


Figure S29. Calculated frontier molecular orbital diagram of Cl-Nb(*i*PrNPh₂)₃Cu-Br (**5**).

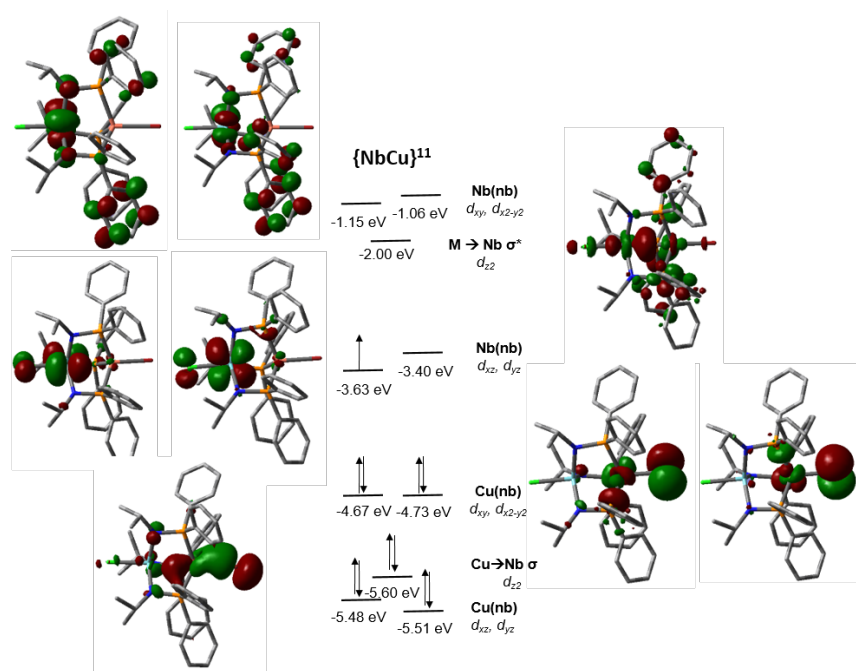


Table S4. Calculated XYZ coordinates for all atoms in **4**.

Symbol	X	Y	Z
Nb	-0.00021	0.000372	1.551551
Ni	0.000497	-0.00057	-0.81799
Cl	-0.00072	0.002988	4.00044
Cl	0.005238	-0.00245	-3.14667
P	-0.97141	-1.93781	-0.18748
P	2.164704	0.12684	-0.18722
P	-1.19344	1.810049	-0.18861
N	-0.9234	-1.85103	1.515853
N	2.065592	0.126016	1.516067
N	-1.14388	1.724517	1.514846
C	-2.73802	-2.21056	-0.64312
C	-3.774	-1.63301	0.139228
H	-3.51705	-1.03934	1.023085
C	-5.12759	-1.81178	-0.21848
H	-5.91537	-1.3652	0.399683
C	-5.46611	-2.55274	-1.37687
H	-6.51763	-2.69234	-1.65427
C	-4.43816	-3.10452	-2.17929
H	-4.68851	-3.6705	-3.08456
C	-3.08188	-2.93369	-1.81833
H	-2.2959	-3.36761	-2.44641
C	-0.1426	-3.4527	-0.85821
C	-0.40075	-4.76134	-0.35856
H	-1.09803	-4.91567	0.471801
C	0.218695	-5.88689	-0.94624
H	0.012513	-6.88788	-0.54851
C	1.086952	-5.72384	-2.05483
H	1.560014	-6.59918	-2.51598
C	1.330927	-4.42933	-2.56829
H	1.992817	-4.29047	-3.43064
C	0.725522	-3.29784	-1.97202
H	0.900496	-2.29624	-2.3852
C	-1.39986	-2.9305	2.447732
H	-1.94347	-3.66643	1.820281
C	-2.41272	-2.42395	3.502984
H	-1.94572	-1.70437	4.194532
H	-2.78269	-3.28457	4.093659
H	-3.28106	-1.94225	3.021169
C	-0.19147	-3.63334	3.113159
H	0.50263	-4.02805	2.349583

H	-0.53379	-4.47476	3.7465
H	0.355279	-2.91689	3.751656
C	3.284785	-1.26555	-0.64505
C	4.073038	-1.20292	-1.82711
H	4.047577	-0.30738	-2.45788
C	4.899829	-2.29037	-2.19127
H	5.507584	-2.22498	-3.1017
C	4.946618	-3.45374	-1.3853
H	5.593912	-4.29324	-1.66525
C	4.145248	-3.53013	-0.22024
H	4.160342	-4.43369	0.400659
C	3.312699	-2.44899	0.140677
H	2.677039	-2.52297	1.029537
C	3.061753	1.60224	-0.85875
C	4.324647	2.032658	-0.36015
H	4.807369	1.505906	0.469918
C	4.989487	3.131701	-0.94834
H	5.959946	3.453305	-0.55151
C	4.413435	3.802359	-2.0564
H	4.935008	4.649428	-2.51805
C	3.169645	3.367042	-2.56862
H	2.71773	3.871225	-3.43037
C	2.492564	2.277244	-1.97171
H	1.536914	1.928623	-2.3837
C	3.238859	0.255643	2.44747
H	4.147906	0.15267	1.819967
C	3.242917	1.65483	3.110568
H	3.236798	2.451882	2.345495
H	4.143211	1.780855	3.74289
H	2.349519	1.770676	3.749616
C	3.307786	-0.87305	3.504637
H	2.4477	-0.83166	4.192096
H	4.234923	-0.75787	4.099184
H	3.331532	-1.86669	3.024666
C	-0.54833	3.477159	-0.6447
C	-1.00086	4.133265	-1.82247
H	-1.76737	3.666986	-2.45138
C	-0.47204	5.393387	-2.18487
H	-0.8357	5.890557	-3.09212
C	0.516553	6.011384	-1.38127
H	0.920432	6.991865	-1.65996
C	0.98708	5.351225	-0.22013
H	1.765303	5.812907	0.399032

C	0.466714	4.089317	0.138903
H	0.851364	3.572885	1.024891
C	-2.91863	1.846861	-0.86278
C	-3.21274	1.020597	-1.98047
H	-2.42974	0.371781	-2.39355
C	-4.49373	1.060079	-2.58033
H	-4.69989	0.419851	-3.44558
C	-5.49709	1.913443	-2.06659
H	-6.49044	1.939951	-2.53051
C	-5.21016	2.743533	-0.95394
H	-5.97746	3.418362	-0.55577
C	-3.92732	2.719264	-0.36251
H	-3.71738	3.397414	0.471457
C	-1.84123	2.677558	2.445577
H	-2.208	3.514867	1.816907
C	-3.05318	1.982856	3.113137
H	-3.74183	1.576227	2.350846
H	-3.6114	2.701342	3.744353
H	-2.70514	1.153489	3.754209
C	-0.89617	3.304317	3.499273
H	-0.50292	2.541317	4.190133
H	-1.45752	4.053698	4.090635
H	-0.04691	3.817511	3.016019

Table S5. Calculated coordinates for all atoms in **5**.

Nb	-0.01212	0.070105	1.857274
Cu	0.024133	0.002381	-0.90232
P	-1.21079	1.838737	-0.11434
N	-0.9698	1.878916	1.577929
C	-1.24874	3.09513	2.427586
C	0.063173	3.64091	3.040865
C	-2.32673	2.826885	3.505165
C	-0.68167	3.442245	-0.8712
C	-1.42031	4.647334	-0.68453
C	-0.97242	5.857736	-1.25863
C	0.210019	5.879157	-2.04003
C	0.930827	4.681774	-2.2547
C	0.487054	3.469678	-1.67589
C	-3.03298	1.846781	-0.41159
C	-3.91817	1.280901	0.543522
C	-5.30708	1.22797	0.290722
C	-5.82836	1.725781	-0.92758
C	-4.9481	2.264345	-1.89798
C	-3.55808	2.318998	-1.64701
P	-1.02046	-1.92938	-0.08351
N	-0.99027	-1.74597	1.614406
C	-1.63715	-2.74887	2.542025
C	-0.70274	-3.25197	3.668651
C	-2.95038	-2.16492	3.117272
C	-0.23359	-3.5615	-0.45323
C	0.795224	-4.07232	0.382647
C	1.437221	-5.29084	0.070497
C	1.07676	-6.00699	-1.09624
C	0.074147	-5.48937	-1.95222
C	-0.57643	-4.27466	-1.63584
C	-2.73374	-2.18945	-0.74731
C	-3.16654	-1.35159	-1.80915
C	-4.44052	-1.53697	-2.39678
C	-5.30042	-2.55602	-1.92757
C	-4.87345	-3.4043	-0.87515
C	-3.59666	-3.22991	-0.29701
Br	0.015123	0.070165	-3.32181
P	2.225456	0.083433	-0.10473
N	2.044238	0.024789	1.596856
C	3.229818	-0.15602	2.513674
C	3.249092	0.846911	3.691451
C	3.285363	-1.61706	3.023106
C	3.296539	-1.27906	-0.77257

C	4.659211	-1.45779	-0.39716
C	5.43148	-2.49357	-0.96777
C	4.861658	-3.35225	-1.94173
C	3.519206	-3.16325	-2.34214
C	2.739988	-2.13543	-1.75973
C	3.269379	1.561966	-0.485
C	3.321773	2.666002	0.406289
C	4.063576	3.822581	0.076911
C	4.747532	3.900615	-1.16001
C	4.678231	2.814575	-2.06761
C	3.943685	1.653414	-1.73551
Cl	-0.12829	0.125779	4.24766
H	-1.64272	3.875235	1.748678
H	-0.13731	4.57332	3.602941
H	0.794105	3.866065	2.24322
H	0.505489	2.906768	3.738137
H	-2.48948	3.74463	4.103204
H	-3.28767	2.545536	3.040623
H	-2.01257	2.021379	4.190457
H	-2.36427	4.637801	-0.12644
H	-1.55111	6.77676	-1.10694
H	0.55375	6.817941	-2.49071
H	1.831565	4.679935	-2.87844
H	1.021102	2.53735	-1.88617
H	-3.51694	0.882418	1.482003
H	-5.97943	0.794657	1.040758
H	-6.90676	1.68783	-1.12183
H	-5.34076	2.643422	-2.84916
H	-2.88598	2.733553	-2.40716
H	-1.87915	-3.63525	1.921113
H	-1.21534	-4.05594	4.231836
H	-0.45142	-2.44593	4.377166
H	0.233066	-3.66892	3.257721
H	-3.46659	-2.91499	3.747753
H	-3.63289	-1.86017	2.304075
H	-2.72612	-1.28194	3.743396
H	1.094877	-3.51124	1.273904
H	2.223223	-5.67497	0.731519
H	1.574492	-6.9534	-1.3385
H	-0.20622	-6.0305	-2.86389
H	-1.35355	-3.88817	-2.30489
H	-2.49159	-0.57962	-2.19941
H	-4.75131	-0.88407	-3.2201
H	-6.2883	-2.69796	-2.38212
H	-5.52614	-4.20858	-0.51483

H	-3.27192	-3.92435	0.485691
H	4.138019	0.043997	1.909961
H	4.189338	0.721651	4.262981
H	3.205857	1.890292	3.332733
H	2.403052	0.676497	4.377368
H	4.176075	-1.7755	3.661598
H	2.385013	-1.83855	3.62603
H	3.331309	-2.32539	2.176618
H	5.13262	-0.77638	0.319278
H	6.478162	-2.61965	-0.66559
H	5.465062	-4.14966	-2.39197
H	3.072541	-3.80684	-3.10835
H	1.710786	-1.97068	-2.10059
H	2.777818	2.61583	1.355403
H	4.102555	4.662117	0.781381
H	5.324612	4.797214	-1.41558
H	5.197576	2.867835	-3.032
H	3.899584	0.81959	-2.44562

References

1. Bruker *Saint*; *SADABS*; *APEX3*., Bruker AXS Inc.: Madison, Wisconsin, USA, 2012.
2. Sheldrick, G. M., *Acta Cryst.* **2015**, *A71*, 3-8.
3. Dolomanov, O. V.; Bourhis, L. J.; Gildea, R. J.; Howard, J. A. K.; Puschmann, H., OLEX2: a complete structure solution, refinement and analysis program. *J. Appl. Crystallogr.* **2009**, *42* (2), 339-341.
4. Spek, A., PLATON SQUEEZE: a tool for the calculation of the disordered solvent contribution to the calculated structure factors. *Acta Crystallographica Section C* **2015**, *71* (1), 9-18.
5. *Apex 2: Version 2 User Manual, M86-E01078*. Bruker Analytical X-ray Systems: Madison, WI, 2006.
6. Altomare, A.; Cascarano, G.; Giacovazzo, C.; Guagliardi, A.; Burla, M. C.; Polidori, G.; Camalli, M., SIR92 - a program for automatic solution of crystal structures by direct methods. *J. Appl. Crystallogr.* **1994**, *27* (3), 435.
7. Betteridge, P. W.; Carruthers, J. R.; Cooper, R. I.; Prout, K.; Watkin, D. J., CRYSTALS version 12: software for guided crystal structure analysis. *J. Appl. Crystallogr.* **2003**, *36*, 1487.
8. Prout, C. K.; Pearce, L. J., Cameron. Cambridge Crystallography Laboratory: Oxford, UK, 1996.
9. Cooper, R. I.; Thompson, A. L.; Watkin, D. J., CRYSTALS enhancements: dealing with hydrogen atoms in refinement. *J. Appl. Crystallogr.* **2010**, *43* (5 Part 1), 1100-1107.
10. Setty, V. N.; Zhou, W.; Foxman, B. M.; Thomas, C. M., Subtle Differences Between Zr and Hf in Early/Late Heterobimetallic Complexes with Cobalt. *Inorg. Chem.* **2011**, *50* (10), 4647-4655.
11. Palatinus, L.; Chapuis, G., SUPERFLIP - a computer program for the solution of crystal structures by charge flipping in arbitrary dimensions. *J. Appl. Cryst.* **2007**, *40*, 786-790.
12. Frisch, M. J. T., G. W.; Schlegel, H. B.; Scuseria, G. E.; Robb, M. A.; Cheeseman, J. R.; Scalmani, G.; Barone, V.; Mennucci, B.; Petersson, G. A.; Nakatsuji, H.; Caricato, M.; Li, X.; Hratchian, H. P.; Izmaylov, A. F.; Bloino, J.; Zheng, G.; Sonnenberg, J. L.; Hada, M.; Ehara, M.; Toyota, K.; Fukuda, R.; Hasegawa, J.; Ishida, M.; Nakajima, T.; Honda, Y.; Kitao, O.; Nakai, H.; Vreven, T.; Montgomery, Jr., J. A.; Peralta, J. E.; Ogliaro, F.; Bearpark, M.; Heyd, J. J.; Brothers, E.; Kudin, K. N.; Staroverov, V. N.; Kobayashi, R.; Normand, J.; Raghavachari, K.; Rendell, A.; Burant, J. C.; Iyengar, S. S.; Tomasi, J.; Cossi, M.; Rega, N.; Millam, J. M.; Klene, M.; Knox, J. E.; Cross, J. B.; Bakken, V.; Adamo, C.; Jaramillo, J.; Gomperts, R.; Stratmann, R. E.; Yazyev, O.; Austin, A. J.; Cammi, R.; Pomelli, C.; Ochterski, J. W.; Martin, R. L.; Morokuma, K.; Zakrzewski, V. G.; Voth, G. A.; Salvador, P.; Dannenberg, J. J.; Dapprich, S.; Daniels, A. D.; Farkas, Ö.; Foresman, J. B.; Ortiz, J. V.; Cioslowski, J.; Fox, D. J. Gaussian, Inc., Wallingford CT, 2009.